Responsive microgel-based inks for inkjet printing:

Application for in-situ sensing on-a-chip

T.J. Lugtmeijer

Delft University of Technology

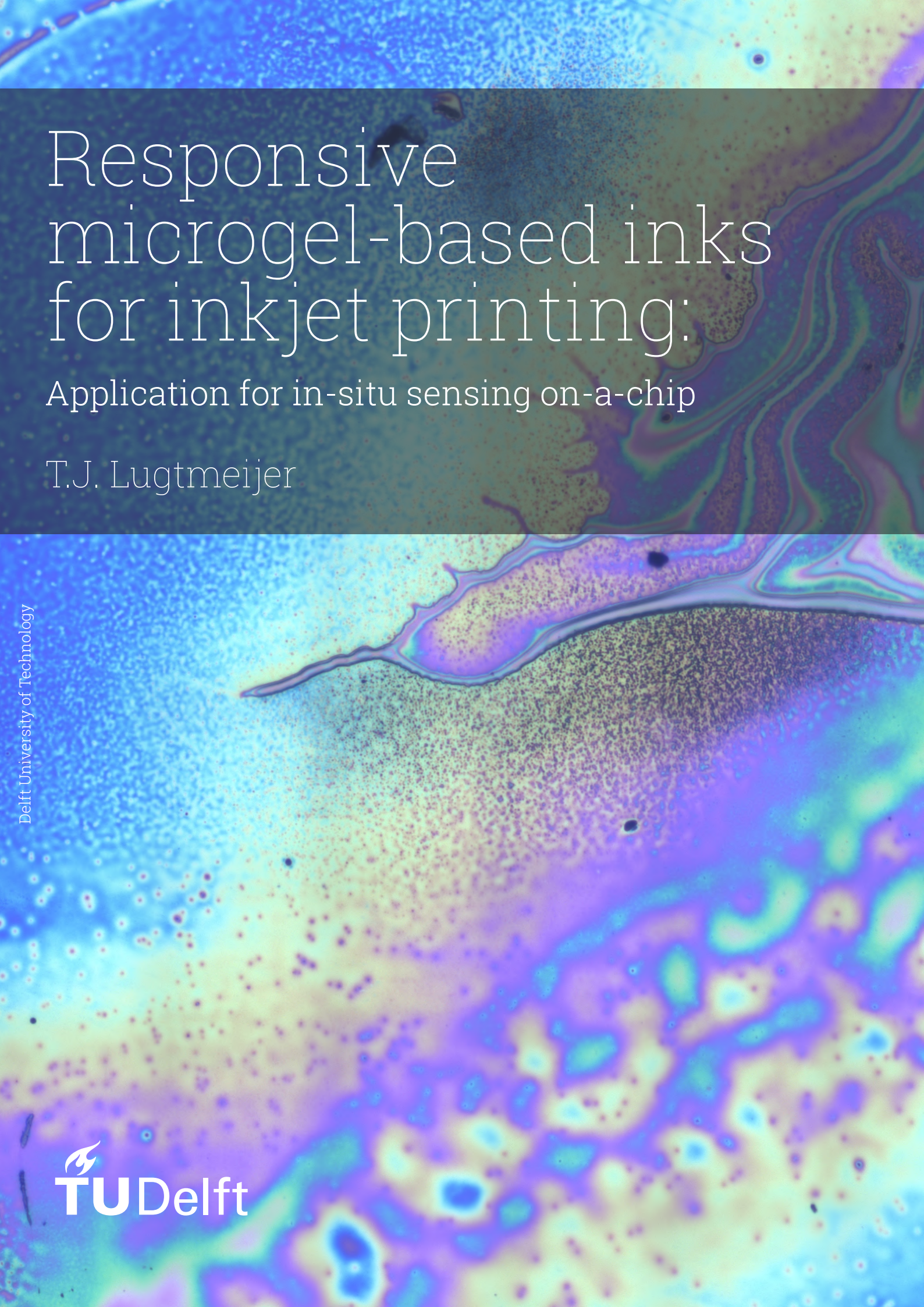

Responsive microgel-based inks for inkjet printing:

Application for in-situ sensing on-a-chip

by

T.J. Lugtmeijer

Student number: 4976983
Project duration: February 1, 2023 – April 15, 2024
Supervisors: Dr. H. Bazyar, G. Kontaxi
Thesis Committee: Dr. H.B. Eral, Dr. A. Hunt

TU Delft

Acknowledgements

The first two people I have to show my appreciation and gratitude to are Dr. H. Bazyar and G. Kontaxi for giving me the opportunity to apply my skills in practice. With their knowledge and technical expertise they enriched my skill set.

A special thanks to Prof. Dr. M. Serpe and Nicholas from the University of Alberta. Their contribution was crucial for understanding the characteristics of pNIPAm. To get a better understanding on how an inkjet printer works both Dr. A. Hunt and Kai knowledge's were essential. Without their input and guidance the quality of the results would have been lower. I would like to thank Chayenne for helping me during my project; the most memorable was her help during my time in the cleanroom, which in there I was like a fish out of water.

Special thanks to my friends. They all greatly supported me in different ways but the one common demominator was that they all provided laughs and entertainment throughout my journey. In no particular order; Animesh, Fathaah, Vignesh, Georgia, Ankit, Mayank, Chayenne, Akhilesh, Kate, Dr. Thanos, Irem, Giuseppe, Ian, David, Jan, Joshua, Panji, Jullien, Neeha, Hannah, Monique, Sridharen, Robin, Martijn, Anna, Nikilesh, Peter and Dr. Mengmeng.

To end with a mantra that helped me during my journey.

"Don't Panic",
Douglas Adams, The Hitchhiker's Guide to the Galaxy

T.J. Lugtmeijer,
April 2024

Abstract

Inkjet printing is a technology that has been widely studied and implemented. The liquids that are used for inkjet printing can vary. There is the traditional ink which can be found in almost every household printer. But it is also possible to use inkjet printing to deposit drugs, proteins and nanoparticles on substrates. Inkjet printing has the ability to precisely deposit picoliters of liquid onto the substrate. Thus, reducing cost and waste when the material being used is expensive and/or of limited quantity. This project works with a LP50 PIXDRO inkjet printer. Another interest that gained traction in the scientific community are the stimuli-responsive microgels. These microgels are able to change their dimensions depending on the external stimuli and if this stimuli is removed from the microgel, it changes back to its original shape, thus it is a reversible process.

This project uses a suspension of the stimuli-responsive microgel; poly(N-isopropylacrylamide)-co-acrylic acid (pNIPAm). This microgel is responsive to temperature and pH. To deposit the pNIPAm suspension on the substrate, inkjet technology will be used. The printability of the pNIPAm will be determined by characterizing the physical and rheological properties. Such as the density, surface tension, viscosity and particle size of the pNIPAm beads. These properties will be compared to the ideal liquid requirements given by the print cartridge that will be used, a Fuijifilm Dimatix. To influence the surface tension three surfactants will be tested. These surfactants are Triton X-114 (TRT), Sodium dodecyl sulphate (SDS) and Hexadecyltrimethylammonium bromide (CTAB). Based on the results the and comparison to the requirements the surfactant Triton X-114 is chosen because it lowers the surface tension the most. While it has minimal to no affect on the pNIPAm particles.

The next phase of the project is testing the printability of the pNIPAm. This is done by adjusting the waveform on the LP50 PIXDRO inkjet printer. As a result it is indeed possible to deposit pNIPAm on a substrate with an inkjet printer. After this step a SEM is used to investigate if the printed pNIPAm particles will form a monolithic layer. This monolithic layer is important when it comes to having a functional etalon. The pNIPAm particles form indeed a monolithic layer on the substrate. The last step is to see if there is a peak shift in the wavelength when the temperature is increased. The microgel based etalons that used an inkjet printer to deposit the micrgol show a peak shift. Therefore, it can be concluded that it is possible to use an inkjet printer to deposit pNIPAm on a substrate and that the pNIPAm particles behave according to literature. All the results of this project show that using an inkjet printer is a viable alternative for fabricating microgel based etalons.

Contents

Acknowledgements i

Abstract ii

Nomenclature ix

1 Introduction 1
- 1.1 Microgel . . . 1
- 1.2 Inkjet printing . . . 1
  - 1.2.1 A brief history on inkjet printing . . . 1
  - 1.2.2 Industries that use inkjet printing . . . 2
  - 1.2.3 Working principle of inkjet printing . . . 2
- 1.3 Research Gap . . . 2
- 1.4 Research Objective . . . 3
- 1.5 Thesis outline . . . 4

2 Methodology: Materials and Equipment 5
- 2.1 Inkjet Printer . . . 5
  - 2.1.1 Surfactants . . . 6
- 2.2 Dimensionless number for printable fluids . . . 6
- 2.3 Microgel Based Etalon . . . 7
  - 2.3.1 Monolithic layer . . . 7
  - 2.3.2 Etalon fabrication . . . 7
  - 2.3.3 Imaging and quality check . . . 8
  - 2.3.4 Reflectance Spectroscopy . . . 8
- 2.4 pNIPAm Characterisation . . . 9
  - 2.4.1 Density . . . 9
  - 2.4.2 Surface Tension . . . 10
  - 2.4.3 Viscosity . . . 10
  - 2.4.4 Particle size . . . 10
  - 2.4.5 Zeta Potential . . . 11

3 Results & Discussion: Microgel Characterisation 12
- 3.1 Microgel Characterisation results . . . 12
  - 3.1.1 Density . . . 12
  - 3.1.2 Surface Tension . . . 13
  - 3.1.3 Viscosity . . . 14
  - 3.1.4 Particle size . . . 18
  - 3.1.5 Zeta Potential . . . 18
  - 3.1.6 Which surfactant? . . . 19
  - 3.1.7 Ohnesorge, Reynolds and Weber Number . . . 19
- 3.2 Printing . . . 21
  - 3.2.1 Print settings . . . 21
  - 3.2.2 Print results . . . 23
  - 3.2.3 Cleaning of the cartridge . . . 29
- 3.3 Inkjet printed sample compared with spincoated sample . . . 29
  - 3.3.1 Print Consistency . . . 30
  - 3.3.2 Gold/white spot removal . . . 31
- 3.4 Reflectance spectroscopy results . . . 32

4 Conclusion 34

5 Recommendations **36**
5.1 pNIPAm INK and Inkjet printing 36
5.2 Application of the inkjet printed pNIPAm 36

References **37**

A Appendix A **41**

List of Figures

1.1 First mass market inkjet printer [7]. 1
1.2 Inkjet printing technique classifications [10]. 2
1.3 Figure *a* shows the schematics of a continuous inkjet printer. The printhead produces a continuous stream of drops. These drops are charged by the electrode. When the drops fall between the deflection plates, the charged drops deviate there trajectory and fall on the substrate. The drops that are not charged, fall into the gutter before they arrive again in the the print head. Figure *b* gives the schematic for the Drop-On-Demand inkjet printer. The printhead uses a piezoelectric transducer to create the drops. How the transducer reacts depends on the waveform that is been used. After a drop is formed they fall onto the substrate. 3

2.1 LP50 PIXDRO [13]. 5
2.2 Diagram of the operating regime for stable drops. When the Ohnesorge number is higher that 1 the ink can be considered too viscous. As a result the cartridge is unable to create drops. When the Ohnesorge number is below $0,1$ the drops produce satellite drops. The No Drop Formation line like the names suggest is the region where there is insufficient kinetic energy to eject a drop. This line is determined by *Derby,2010*[27] to be We ≥ 4. The splashing region is determined by *Derby,2010*[27] to be $OhRe^{5/4} \geq 50$. 7
2.3 Schematic of a non monolithic layer (*a*). When there is a non monolithic layer of the pNIPAm particles the etalon mirrors are not parallel to each other. This causes the measured reflectance spectrum to be inaccurate. When the pNIPAm particles form a monolithic layer like in *b*. The mirrors are parallel from each other. This means the the measuered reflectance spectrum is accurate. 8
2.4 Schematic of the pendant drop method, used for measuring the surface tension of pNIPAm, pNIPAm-TRT, pNIPAm-CTAB and pNIPAm-SDS. The light source creates a shadow of the drop which the camera registers. The software calculates the surface tension based on the Young-Laplace equation. 10

3.1 This graph shows the average of three measurements the pNIPAm, pNIPAm-TRT, pNIPAm-CTAB and pNIPAm-SDS density ($g/cm3$) vs the temperature (°C). It shows that adding the surfactants SDS and CTAB does not affect the density of pNIPAm compared to the without any added surfactants. However, adding TRT to the suspension does have an effect on the density when the LCST is approached. 12
3.2 The graph shows the average surface tension of ten measurements of pNIPAm, pNIPAm-TRT, pNIPAm-CTAB and pNIPAm-SDS vs Temperature (°C). It can be seen that the surface tension decreases when the surfactants are added to the pNIPAm suspension. Also, that it decreases when the temperature increases. Of the three surfactants used Triton X-114 lowers the surface tension the most. The standard deviation is determined by three measurements taken at each temperature. 13
3.3 Shear Stress vs Shear Rate of pNIPAm (*a*), pNIPAm-TRT (*b*), pNIPAm-CTAB (*c*) and pNIPAm-SDS (*d*) at temperatures 20,30 and 35°C. As can be seen in *a,b,c* and *d* the measured shear stress lowers when the temperature decreases. The standard deviation shown is determent by two measurements. 14
3.4 Viscosity vs Shear Rate of pNIPAm (*a*), pNIPAm-TRT (*b*), pNIPAm-CTAB (*c*) and pNIPAm-SDS (*d*) at temperatures 20,30 and 35°C. It shows in *a,b,c* and *d* that when the temperature increases the viscosity deceases. The standard deviation shown is determent by two measurements. 15

3.5 *a*, *c* and *e* shows the Shear stress vs Shear rate at 20,30 and 35°C of pNIPAm, pNIPAm-TRT, pNIPAm-CTAB and pNIPAm-SDS. At high shear rate the added surfactants have little influence on the measured shear stress. Figures *b*, *d* and *f* compares the Viscosity vs Shear rate at 20, 30 and 35°C for pNIPAm, pNIPAm-TRT, pNIPAm-CTAB and pNIPAm-SDS. The added surfactants have no meaningful influence on the viscosity at a shear rate of $10000\ 1/s$. The values shown in the graph represent the average taken from two measurements. 17
3.6 Particles size (nm) of pNIPAm, pNIPAm-TRT, pNIPAm-CTAB and pNIPAm-SDS vs Temperature (°C). Adding surfactants have minimal influence one the size of the pNIPAm particles. Each data point in the graph is an average of three measurements. As the literature suggests, the pNIPAm particles decrease in size when the temperature is increases. 18
3.7 Diagram of the operating regime for stable drops. The dots blue (20°C), green (30°C) and red (35°C) show that using the calculated velocity will not result in pNIPAm-TRT drop formation. 20
3.8 (*a*) shows a schematic of a Waveform for inkjet printing. (*b*) shows the waveform that is used to jet the pNIPAm. (*c*) shows the drop velocity and drop volume. The arrow represents the angle in which the drop is falling. Ideally this angly should be 0°because that means the the drop jets straight. (*d*) shows the dots blue (20°C), green (30°C) and red (35°C) using the measured velocity. Of theses three temperatures, the 20°C, is the only temperature what is in the printable area. While the other two, 30°C and 35°C are in the regime where satellite drops can be formed. 22
3.9 (*a*)Optical microscope image showing a print of 500 DPI. The shaded roster is caused by the microscope and is not present on the actual print. (*b*) SEM image of a 500 DPI print at 1000x magnification, (*c*) SEM image 4000x magnification, (*d*) SEM image 10000x magnification of a printed pNIPAm-TRT sample at a DPI of 500 and (*e*) shows the drop size and spacing between each drop. 24
3.10 *a)* Optical microscope image showing a print of 1500 DPI, (*b*), (*c*) and (*d*) are SEM images at 1000x, 4000x and 10000x magnification of a printed pNIPAm-TRT sample at a DPI of 1500. The SEM pictures are taken in the blue area of the print. It shows that a monolithic layer is formed of the pNIPAm particles. 25
3.11 *a)* Optical microscope image showing a print of 2000 DPI, (*b*), (*c*) and (*d*) are SEM images at 1000x, 4000x and 10000x magnification of a printed pNIPAm-TRT sample at a DPI of 2000. All the images show that a monolithic layer of pNIPAm particles is achieved. . . . 26
3.12 *a)* Optical microscope image showing a print of 4000 DPI, (*b*), (*c*) and (*d*) are SEM images at 1000x, 1000x and 40000x magnification of a printed pNIPAm-TRT sample at a DPI of 2000. All the images show that a monolithic layer of pNIPAm particles is achieved. . . . 27
3.13 *a)* Optical microscope image showing a print of 1500 DPI 2 iterations, (*b*), (*c*) and (*d*) are SEM images at 500x, 1000x and 4000x magnification of a printed pNIPAm-TRT sample at a DPI of 1500 2 iterations. In *b* it shows that there appear to be two layers of pNIPAm particles, because of the two iterations of printing, but it still appears to be monolithic. However, *c* and *d* show a hill like structures. Thus implying a non monolithic layer. . . . 28
3.14 Clean nozzle (*a*) before use, (*b*) shows the nozzle after use. It can be seen that the area is covered with pNIPAm particles. It is therefore needed to clean the nozzle after each use. To clean the nozzle a sonicator for 2 minutes is used as seen in*c*. 29
3.15 SEM image of (*a*) Spincoated pNIPAm with Triton X-114 and (*b*) Inkjet printed pNIPAm with Triton X-114. 29
3.16 Print quality of $3\ mm$ samples with DPI of 1500(*a,b,c*), 2000(*d,e,f*) and 4000(*g,h,i*). At 1500 DPI the difference in quality is the most noticeable. There is no consistency where there is no pNIPAm deposit. Same can be said for the 2000 DPI. However, the consistency is more noticable. The gold substrate is more covered compared to the 1500 DPI. The 4000 DPI covers the substrate the best and shows the most consistency amongs the three different DPI's. 30

3.17 In (*a*) the sample, the residual water is removed by a tip of tissue paper. (*b*) the residual water is removed by blowing argon of the deposited pNIPAm-TRT. It shows that the majority of the gold/white is removed using this method. The last method (*d*) was putting the sample in a small petri dish and fill it with Milli-Q® and slowly remove the water by tilting the petri dish until all the water is removed. This methods shows that the drop in (*c*) is almost completely removed. 31
3.18 Reflectance spectroscopy results of the peak shift. (*a*) 1500 DPI, (*b*) 1500 DPI 2 iterations, (*c*) 2000 DPI and (*d*) 4000 DPI. They all show a decrease in $\Delta\lambda$. This due to the fact that the pNIPAm particles deswell when the temperature increases. When the temperature reaches 45°C and up, a plateau is reached. Because the pNIPAm particles do not deswell further beyond this point. 33

A.1 Zetapotential of pNIPAm, pNIPAm-TRT pNIPAm-SDS and pNIPAm-CTAB. 42
A.2 $3\ mm$ diameter print at 500 DPI. 43
A.3 PNIPAM applied by spincoating. 44
A.4 PNIPAM + Triton X114 applied by spincoating. 44
A.5 PNIPAM + SDS applied by spincoating. 45
A.6 PNIPAM + CTAB applied by spincoating. 45
A.7 pNIPAm density difference on the border of a gold/white spot. 46
A.8 Result of trial and error in finding the right waveform. 46
A.9 Result of trial and error in finding the right waveform. 47
A.10 Result of trial and error in finding the right waveform. 47
A.11 1500 DPI Normalized intensity vs Wavelength. 48
A.12 1500 DPI Normalized reflection vs Wavelength. 48
A.13 2000 DPI Normalized intensity vs Wavelength. 49
A.14 2000 DPI Normalized reflection vs Wavelength. 49
A.15 4000 DPI Normalized intensity vs Wavelength. 50
A.16 4000 DPI Normalized reflection vs Wavelength. 50
A.17 1500 DPI 2 iterations Normalized intensity vs Wavelength. 51
A.18 1500 DPI 2 iterations Normalized reflection vs Wavelength. 51

List of Tables

2.1 List of characteristics of ideal fluid requirements for the *Dimatix® Materials Cartridge - Samba® Cartridge* as suggested by *Fuijfilm* used in the *LP50 PiXDRO*. 5

2.2 The samples are made by starting with a pNIPAm base concentration of $47,9\ mg/ml$. Of each surfactant a dilution is made based on the CMC level. After which four samples are made with an end concentration of $42,57\ mg/ml$. Sample one, pNIPAm; is $1\ ml$ pNIPAm diluted with $1,25\ ml$ Milli-Q® water, sample two, pNIPAm-TRT; pNIPAm diluted with $1,25\ ml$ Milli-Q® water plus $4,7\ \mu l$ of TRT, sample three, pNIPAm-CTAB; pNIPAm diluted with $1,25\ ml$ Milli-Q® water plus $6,7\ \mu l$ of CTAB and sample four, pNIPAm-SDS; pNIPAm diluted with $1,25\ ml$ Milli-Q® water plus $22,8\ \mu l$ of SDS 9

2.3 Zeta Potential and stability [44]. The zeta potential gives an insight on the stability of the pNIPAm beads in the suspension. It shows the repulsion between each charged particle. When this is low, there is a change that the particles flucculate. But when the zeta potential is high, it means that the particles are desperesed well enough to avoid aggragation. 11

3.1 Density ρ (g/cm^3) of pNIPAm, pNIPAm-TRT, pNIPAm-CTAB and pNIPAm-SDS at temperatures 20,30 and 35°C. This table shows that the density decreases when the temperature increases. The standard deviation is determined by three measurements taken at each temperature. 13

3.2 Surface Tension γ (mN/m) of pNIPAm, pNIPAm-TRT, pNIPAm-CTAB and pNIPAm-SDS at temperatures 20,30 and 35°C. It can been seen that the surface tension for all samples decrease when the temperature increases. Of the three surfactants Triton X-114 lowers the surface tension the most, from $67,44$ till $38,4\ mN/m$. 13

3.3 Measured viscosity of pNIPAm, pNIPAm-SDS, pNIPAm-TRT and pNIPAm-CTAB at a shear rate of $10000\ 1/s$ at 20, 30 and 35°C. At 30 and 35°C, the surfactants have little to no influence on the viscosity. However, at 20°C, there is a noticable difference in the viscosity. It is however not investigated if the surface tension has an relation with the viscosity. 16

3.4 Particles size nm of pNIPAm, pNIPAm-TRT, pNIPAm-CTAB and pNIPAm-SDS at temperatures 20,30, 35 and 45°C. 18

3.5 The Measured Zeta potantial at 45°C. it shows that adding surfactants lowers the overall zeta potential. Of the three surfactants the anionic surfactant SDS lowers the zeta potential the most. While the non-ionic surfactant TRT is in between SDS and CTAB the cationic surfactant. 19

3.6 The measured characteristics of pNIPAm-Triton X114 at shear rate of $10000\ 1/s$ and temperatures 20,30 and 35°C. 19

3.7 The Reynolds, Weber and Ohnesorge Number for pNIPAm-TRT at a temperatures of 20, 30 and 35°C. Given that the requirement is We ≥ 4), indicates that there will be no drop ejected due to the lack of kinetic energy. 19

3.8 The Reynolds, Weber and Ohnesorge Number at a temperature of 20,30 and 35°C calculated with the new measured velocity of $5,70\ m/s$. 23

Nomenclature

Abbreviations

Abbreviation	Definition
Re	Reynolds Number
We	Weber Number
Oh	Ohnesorge Number
DPI	Dots Per Inch
LCST	Lower Critical Solution Temperature
pNIPAm	Poly(N-isopropylacrylamide)
OoC	Organ-On-Chip
TRT	Triton X-114
CTAB	Hexadecyltrimethylammonium bromide
SDS	Sodium Dodecyl Sulphate

Symbols

Symbol	Definition	Unit
U	Velocity	[m/s]
v_{min}	Minimum Velocity	[m/s]
d_n	Nozzle Diameter	[m]
D	Nozzle Diameter	[m]
d	Particle Diameter	[m]
ρ	Density	[kg/m^3]
γ	Surface Tension	[mN/m]
τ	Shear Stress	[Pa]
μ	Dynamic Viscosity	[Pa· s]
λ	Wavelength	[m]
ζ	Zeta Potential	[mV]

1 Introduction

1.1. Microgel

Stimuli-responsive microgels have attracted great scientific interest. The microgels could be considered a "*smart material*" due to their ability to change their dimensions depending on the external stimuli they receive [1]. The thermo-responsive Poly(N-isopropylacrylamide) or pNIPAm polymer is used, its solubility is inverse when it is being heated. This behaviour is the opposite of most polymers in organic solvents [2]. This change from hydrophilic to hydrophobic structure occurs at a temperature range that is known as the Lower Critical Solution Temperature (LCST). This has been experimentally established to be between 30°C. and 35°C. [2]. Being able to change its solubility with temperature, renders it a versatile polymer. Modification of pNIPAm suspensions, during synthesis, render the microgels responsive to other stimuli, for instance pH, ionic strength variations and glucose [3, 4]. With the stimulus removed the polymer should fully reverse to its original state.

1.2. Inkjet printing

There is an increasing need for depositing liquids with micro-precision, liquids such as drugs, proteins and nanoparticles [5, 6]. To deliver these liquids with micro-precision, inkjet printing technology is a promising method. Inkjet printing gives the ability to deposit drops of the ink, in picoliters onto a substrate, with high precision. This precision would reduce the costs and waste when the available material is expensive or in limited quantity.

1.2.1. A brief history on inkjet printing

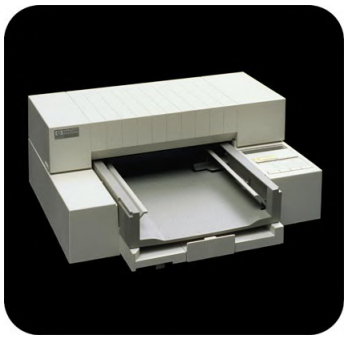

Figure 1.1: First mass market inkjet printer [7].

Inkjet printing and its technology was developed in the early 1950s [8]. It can be said that there is no single inventor when it comes to the invention of inkjet printing. A number of companies worked on the technology at the same time. Companies such as Epson, Hewlett Packard and Canon. At the end of the 1970s inkjet printers were able to produce images created by computers. The first inkjet printers to reach the commercial market was in the late 1980s. The Hewlett Packard's DeskJet printer, as seen

in Figure 1.1, is considered to be the first mass produced inkjet printer for the market, and at the time it would cost $1,000 dollars [7].

1.2.2. Industries that use inkjet printing

Due to its ability to deposit liquids with micro-precision inkjet printing technology has been a method that is being used more and more over the years in various fields. For instance the optoelectronics industry is researching and developing methods to use inkjet printing for the fabrication of their organic light-emitting diodes (OLED) displays [9]. Besides printing OLEDS, inkjet printing is also increasingly being used in the electronics industry to print circuit boards because of its precision and low waste. In the pharmaceutical industry, inkjet printing provides a method of depositing liquids such as drugs, proteins and nanoparticles [5, 6].

1.2.3. Working principle of inkjet printing

Inkjet printers produce and deposits small droplets of a liquid on a substrate. There are various ways of producing these droplets and the most common techniques are; Continuous Inkjet printing (CIJ), Drop-On-Demand (DOD) as shown in Figure 1.2

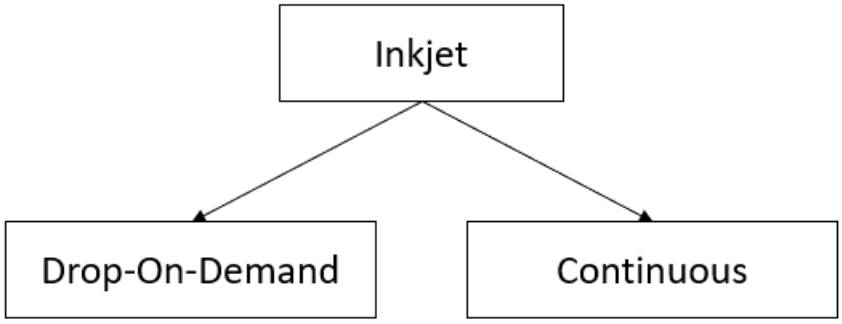

Figure 1.2: Inkjet printing technique classifications [10].

Continuous Inkjet printing

As the name suggest this method uses a continuous jet of ink which is formed by putting it under pressure through the nozzle. The breaking of the jet into drops is driven by surface tension forces, while the spacing and the size of the drops are controlled. Certain drops of the stream are selected to be used for the print this selection is done by the printing signals. An electrode is used to charge these selected drops. Then the stream of drops pass through a deflection plate and the charged drop will deviate and fall onto the substrate. The remaining drops will be caught in and re-used again [10]. This principle is shown in Figure 1.3a

Drop-On-Demand

In contrast to continuous inkjet printing, it is not needed to catch the ink and reuse it or to use a deflection plate for the falling drops. This means that it is possible to position the nozzle of the printhead close to the surface of the substrate. Another difference between continuous inkjet printing and Drop-On-Demand is that there is no continuous stream of drops. The drops are formed by using a driving mechanism that provides enough energy to produce a drop of the used fluid [10]. Figure 1.3b shows a schematic of how Drop-On-Demand printing works with a piezoelectric transducer to provide the driving mechanism.

1.3. Research Gap

Both inkjet printing and pNIPAm microgels are a topic that have been extensively studied. Inkjet printers because of their ability to deposit liquids with microprecision. While pNIPAm is studied for its swelling

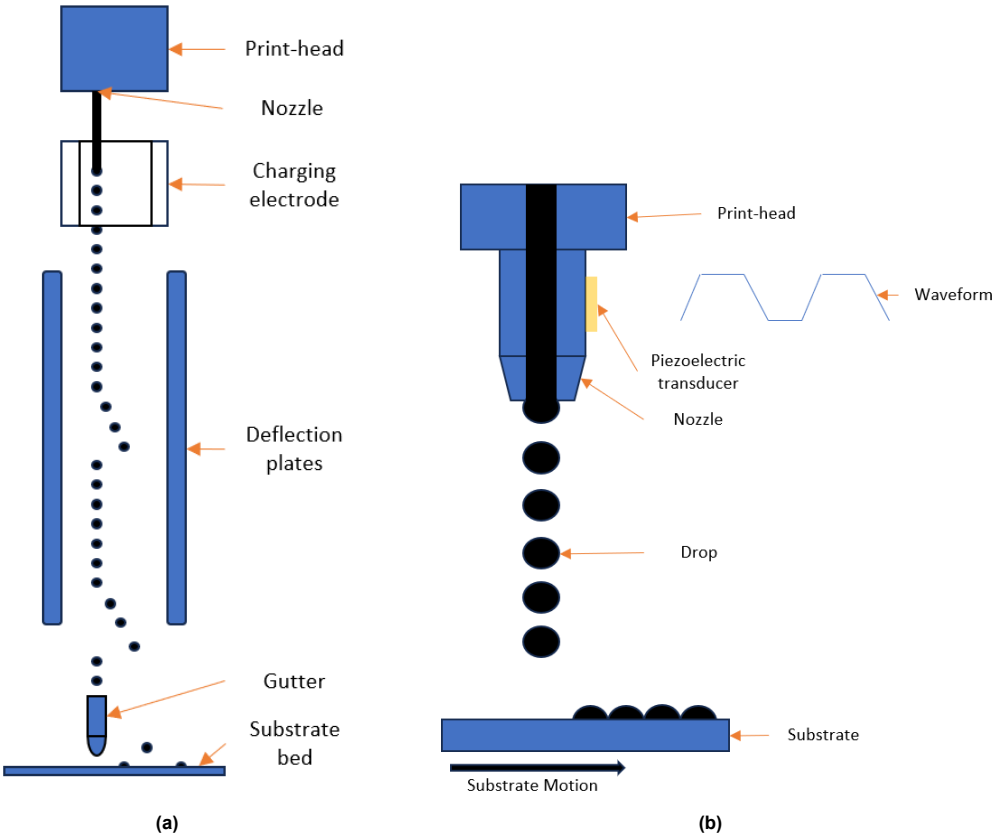

Figure 1.3: Figure *a* shows the schematics of a continuous inkjet printer. The printhead produces a continuous stream of drops. These drops are charged by the electrode. When the drops fall between the deflection plates, the charged drops deviate there trajectory and fall on the substrate. The drops that are not charged, fall into the gutter before they arrive again in the the print head. Figure *b* gives the schematic for the Drop-On-Demand inkjet printer. The printhead uses a piezoelectric transducer to create the drops. How the transducer reacts depends on the waveform that is been used. After a drop is formed they fall onto the substrate.

and deswelling when in contact with outside stimuli. This characteristic creates an opportunity to make microgel based etalons where a shift in wavelength can be measured depending on the state of the microgel. The following gaps have been found when combining the pNIPAm microgel and inkjet printing technology when literature study was conducted in the creation of etalons. These gaps are as follows;

- Depositing pNIPAm on a substrate by the use of inkjet printing. The current methods for making microgel based etalons use either a spincoating or a ”paint-on” method[11, 12].
- Reflectance spectroscopy of microgel based etalons deposited by inkjet printing.

1.4. Research Objective

Hence, the research goal arises is conduction an experimental study on microgel-based inks for inkjet printing. For this scope rheological and physical properties of aqueous pNIPAm suspensions are studied. In particular, density, surface tension, viscosity and particle size measurements are being performed. An inkjet printer designed for Research and Development (R&D) is used to deposit the pNIPAm onto a substrate. Lastly to validate the the printability of pNIPAm and its success, a reflectance spectroscopy measurement is conducted to investigate if there is a shift in the measured peak when the temperature is increased. However, what is outside the scope of this research is both optimising the pNIPAm ”*ink*” and optimising the printer.

1.5. Thesis outline

The project can be devided in three sections. The first section is characterization of the microgel, poly(N-isopropylacrylamide)-co-acrylic acid (pNIPAm) and what the effects are of adding surfactants have on the pNIPAm suspension. This chararacterisation consists of measuring the density, surface tension, viscosity, particle size and zeta potential. The second part is using the inkjet printer to verify if depositing pNIPAm is viable. The last part is conducting reflectance spectroscopy and measure the decrease in peak wavelength when the temperature is increased.

The report is structures as follows;

- Chapter 2: Methodology of Materials and Equipment, and of Characterization of pNIPAm and the added surfactants
- Chapter 3: Results and discussion of the characterization of the pNIPAm, Images of the deposited pNIPAm from inkjet printing and the reflectance spectroscopy results
- Chapter 4: Conclusion
- Chapter 5: Recommendations for further studies or direction this research can be taken in

2

Methodology: Materials and Equipment

2.1. Inkjet Printer

The inkjet printer *LP50 PiXDRO* from *SUSS MicroTec,Germany* with the accompanied software *PIXDRO 4.4.8.4*, seen in Figure 2.1 is used to check the printability of the pNIPAm suspension. The cartridge is a *Dimatix® Materials Cartridge - Samba® Cartridge* (DMC Samba) from *Fuijifilm*. The company of this cartridge provided a list of characteristics as the ideal requirements of a fluid that uses the *Dimatix*. The characteristics are shown in Table 2.1. The pNIPAm microgel suspension has to be adjusted in such a way that it fits or approaches theses ideal requirements.

Table 2.1: List of characteristics of ideal fluid requirements for the *Dimatix® Materials Cartridge - Samba® Cartridge* as suggested by *Fuijifilm* used in the *LP50 PiXDRO*.

Ideal Fluid Requirements Dimatix cartridge	
Viscosity	4-8 $mPas$
Surface Tension	28-32 mN/m
Type	Water-based, Solvent-based, UV Curable, Hybrids
Mixture	Homogeneous, sub-micron particle size
pH	neutral
Stability	Thermally stable for 2 weeks at 60 $°C$ (140$°F$)

Figure 2.1: LP50 PIXDRO [13].

Print precision

Another subject that is important when it comes to inkjet printing, is the effect of the impact of the drop on the substrate. The spreading of the drop, splashing of the drop when it hits the substrate. Thus, reducing the quality of the print. The splashing and spreading of the drop depends on the roughness and type of substrate [14, 15, 16, 17]. The impact angle of the droplet on the substrate also contributes to the shape of the droplet on the substrate affecting the quality of the print [18, 19].

Drying of the drop

The next step would be to let the ink dry. During drying it is possible that the pNIPAm particles will form a structure among the edge of the drop. This phenomena can also be describe as the *Coffee Ring Effect* [20]. This *Coffee Ring Effect* happens due to the fact that the evaporation rate is faster at the

edges than at other parts of the drop, leading to an induced flow in the droplet. This phenomena is also known as the Maragoni Effect. If the flow in the droplet is strong enough, it is capable to move the particles to the edge of the drop. It is therefore important to be able to control the evaporation to keep the overall quality of the print and prevent the build-up of particles along the edges of the drop [21].

2.1.1. Surfactants

It is known that surfactants reduce the interfacial tension between surfaces. Besides lowering the interfacial tension, adding surfactants also have an effect on the contact angle with the substrate [22]. Surfactants have an important influence on various processes when it comes to inkjet printing. The surface tension is important for the droplet jetting, the formation of satellite drops, the impact of the droplet on the substrate, interaction between drops and drop and substrate, and the drying of the droplet [23, 24, 25, 26]. The surfactants that will be used in this report are: Triton X-114 (TRT) *Sigma-Aldrich laboratory grade*, Sodium Dodecyl Sulphate (SDS) *Sigma Aldrich* $\geq 99,0\%$ and Hexadecyltrimethylammonium bromide (CTAB) *Sigma Aldrich* $\geq 98\%$. These are in order mentioned *non-ionic*, *anionic* and *cationic*.

2.2. Dimensionless number for printable fluids

In fluid dynamics the use of dimensionless numbers to express ratios of various forces or scales is utilized to explain behaviour of liquids. These dimensionless numbers are also applicable to inkjet printing. The most relevant ones for inkjet printing and Newtonian fluids are as follows.

Weber Number

The **Weber number** gives the ratio between the inertia and surface tension forces. This is given by Equation:

$$We = \frac{U^2 \rho D}{\gamma}, \tag{2.1}$$

where γ (mN/m) is the surface tension, ρ (g/cm^3) is the density , *U* (m/s) the velocity and *D* (m) a characteristic length.

Reynolds Number

The **Reynolds number** defines the ratio between inertial and viscous forces and is given by Equation:

$$Re = \frac{U \rho D}{\mu}, \tag{2.2}$$

where ρ (kg/m^3) is the density of the fluid, *U* (m/s) is the velocity of the fluid , μ $(mPa \cdot s)$ the viscosity and the D (m) is the characteristic length. In this case it is the diameter of the nozzle.

Ohnesorge Number

Combining the Reynolds number from equation (2.2) and Weber number from equation (2.1) removes the dependency on velocity *U* and gives the **Ohnesorge number** (Oh), which is given by Equation:

$$Oh = \frac{\sqrt{We}}{Re} = \frac{\mu}{\sqrt{\rho \gamma D}}. \tag{2.3}$$

This number shows the ratio between viscous, surface tension and inertia forces. The *Oh* number gives the stability of the drop. These numbers are able to give an inkjet-printable area to produce pNIPAm beads/drops. In Figure 2.2 the plot of Reynolds number vs the Oh number is presented. The No Drop Formation line means the minimum needed kinetic energy to jet a drop. This is determined that the We ≥ 4 by *Derby,2010*[27] and the splashing region criteria is $OhRe^{5/4} \geq 50$ also determined by *Derby,2010*[27]. This figure show that, to have a printable fluid, the Oh number has to be in range of 0.1 and 1 [28], We ≥ 4 and $OhRe^{5/4} \geq 50$.

To form a drop there has to be enough energy to overcome the surface tension thus, a minimum velocity is needed to eject a drop [29]. Equation 2.4 shows the required minimum velocity,

$$v_{min} = \left(\frac{4\gamma}{\rho d_n} \right)^{1/2}, \tag{2.4}$$

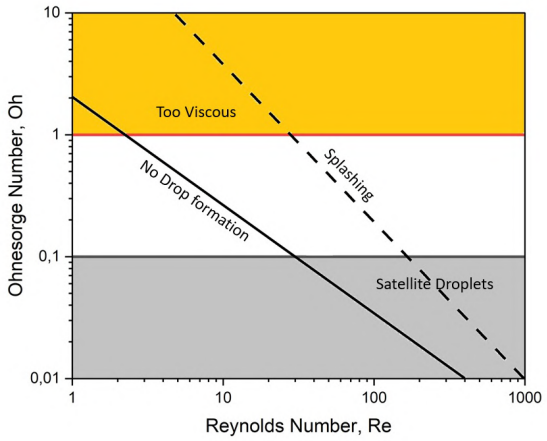

Figure 2.2: Diagram of the operating regime for stable drops. When the Ohnesorge number is higher that 1 the ink can be considered too viscous. As a result the cartridge is unable to create drops. When the Ohnesorge number is below $0,1$ the drops produce satellite drops. The No Drop Formation line like the names suggest is the region where there is insufficient kinetic energy to eject a drop. This line is determined by *Derby,2010*[27] to be We ≥ 4. The splashing region is determined by *Derby,2010*[27] to be $OhRe^{5/4} \geq 50$.

where γ (N/m) is the surface tension, ρ (kg/m^3) the density and d_n (m) the nozzle diameter. To perform the experiment $1\ ml$ of the pNIPAm suspension is used.

2.3. Microgel Based Etalon

An interferometer or etalon is an optical device consisting of two reflective mirrors or surfaces. These two surfaces are separated by a dielectric layer. When light enters the etalon, the difference in contrast between the mirror and the layer causes interference with the light. Besides this difference, the reflective properties of the surfaces also contribute to this interference. This interference can be measured as a reflective spectrum. This spectrum can be described by the *Bragg's Law* as seen in Equation 2.5,

$$m\lambda = 2ndsin\theta. \tag{2.5}$$

Where λ is the wavelength (m) of the peak, m is the peak order, d is the distance between the mirrors $(m\ )$, n is the reflective index of the dielectric layer and θ is the angle of incidence. For this project the layer between the mirrors is a pNIPAm microgel layer. As mentioned in Chapter 1 pNIPAm is thermo-responsive. Thus the swelling and deswelling of the pNIPAm changes the distance between the mirrors when the temperature decreases or increases, which as a result produces a shift in the peak wavelength.

2.3.1. Monolithic layer

Considering the pNIPAm particles swell and deswell depending on the temperature[30] or pH[31], it is important to control the deposition of the particles. If a monolithic layer of the particles is not achieved, see Figure 2.3a, then the distance between the two mirrors are not the same. This means that the measured reflectance spectrum is not accurate. When the particles form a dense monolithic layer, the particles and the two mirrors (represented by gold layers) are almost parallel to each other. Figure 2.3b shows the schematic of a dense monolithic layer of the beads. Thus the measured reflectance spectrum is more accurate.

2.3.2. Etalon fabrication

The fabrication of the etalons is based on the procedures in [32, 11] with some minor adjustments because of location limitations. The paper[32, 11] mentions that the glass coverslips are first rinsed with ethanol and then dried with N_2 gas before the first reflective layer. This is not done during this project. The step of annealing the first Cr/Au substrate at 250°C for three hours was also not done. After removing excess pNIPAm particles of the samples, they were not soaked overnight in Milli-Q® water. The glass coverslips that are used are from *Menzel-Gläser,Germany* of 18 by $18\ mm$. To deposit the

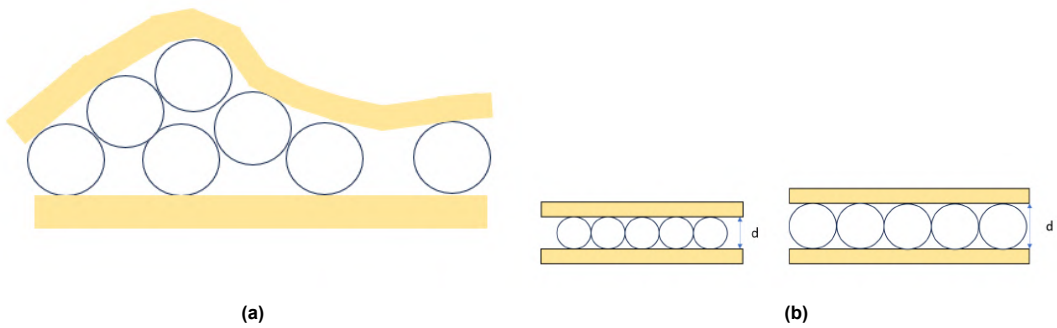

Figure 2.3: Schematic of a non monolithic layer (*a*). When there is a non monolithic layer of the pNIPAm particles the etalon mirrors are not parallel to each other. This causes the measured reflectance spectrum to be inaccurate. When the pNIPAm particles form a monolithic layer like in *b*. The mirrors are parallel from each other. This means the the measuered reflectance spectrum is accurate.

Cr/Au on the glass physical vapor deposition a *CHA's Solution™PLC-S7* from *CHA Industries Inc,USA* is used. The first reflective layer of the etalon is of $2\ nm$ of Chromium followed by a $15\ nm$ layer of Au at a speed of 1 and $3\ As^{-1}$. After the first layer of chromium and gold a $3\ mm$ dot of the pNIPAm will be deposited by the *LP50 PiXDRO* from *SUSS MicroTec* inkjet printer. After printing the samples will be put on a hotplate at 30°C for 1 hour. Followed by rinsing with Milli-Q® water for removing excess pNIPAm particles and dried covered overnight on a hotplate at 30 °C. The next step is to add the second layer of Cr and Au, which as the first layer will have the thickness of $2\ nm$ and $15\ nm$ and will deposited at a rate of 1 and $3\ As^{-1}$.

2.3.3. Imaging and quality check

To be able to check the monolithic layer of the pNIPAm suspension, a scanning electron microscope (SEM) *JSM-6010LA* from *JEOL, Ltd, Japan* with the accompanied software*InTouchScope 1.12* software is used. The SEM will be primarily used for investigating the monolithic layer of the beads. An optical microscope *Nanoro M* and software-version $4.8.103$ from *LIG Nanowise,UK* will be used to check the print quality. The print quality can be determined by checking the following; the overall drop precision, consistency of each drop, how does the drop dry.

2.3.4. Reflectance Spectroscopy

The final step is to check if the inkjet-printed etalons respond to temperature and show a peak shift similar to spin-coated etalons. To measure this peak shift a *Ocean Insight FLAME Miniature Spectrometer, Ocean optics CO, LTD* spectrometer in combination of the company's software *Oceanview 2.0.14* is used. To conduct this experiment the etalon is placed in a glass petri dish. This petri dish is put on a hotplate. The temperature range during this experiment is from 20 till 65°C in steps of 5°C. The data is collected at each temperature after waiting for 20 minutes. This is to assure that the temperature is steady and that the pNIPAm beads have time to adjust to the temperature. The baseline of 20°C is used. The difference in wavelength peak shift at higher temperatures compared to the baseline is considered the $\Delta\lambda$.

Methodology: Characterization of pNIPAm

2.4. pNIPAm Characterisation

The printability of pNIPAm depends on its physical properties. There are several properties that have an influence on the printability. The main properties to be characterized are density (ρ), surface tension (γ) and the viscosity (μ) [33, 34]. When a liquid is a suspension, the particles will also play a role in its printability as they can provoke clogging of the nozzle. These particles can aggregate [35] and influence the printability. Therefore it is important to characterise the particle size of the pNIPAm beads and its stability. To determine the stability, the zeta potential has to be measured. As mentioned, the pNIPAm microgel changes from hydrophilic to hydrophobic around the LCST. Therefore, the characterisation is done at the following temperatures; $20, 25, 30, 32, 33, 34, 35, 36, 40$ and 45°C. As mentioned in Chapter1 the LCST is experimentally established between 30 and 35°C. Hence, the steps taken in this range are smaller. The pNIPAm suspension has to be in range of the given fluid requirements seen in Table 2.1. The used surfactants, Triton X-114 (TRT), Sodium Dodecyl Sulphate (SDS) and Hexadecyltrimethylammonium bromide (CTAB) are *non-ionic*, *anionic* and *cationic*, respectively. The amount of surfactant used is determined by their Critical Michelle Concentration for $10\ ml$ water seen in Table 2.2. These surfactant mixtures are then added to the pNIPAm. The base concentration of pNIPAm is $47,9\ mg/ml$. This is diluted till $42,57\ mg/ml$ for each of the four samples. These samples are;

- pNIPAm; $1\ ml$ pNIPAm diluted with $1,25\ ml$ Milli-Q® water
- pNIPAm-TRT; pNIPAm diluted with $1,25\ ml$ Milli-Q® water plus $4,7\ \mu l$ of TRT
- pNIPAm-CTAB ;pNIPAm diluted with $1,25\ ml$ Milli-Q® water plus $6,7\ \mu l$ of CTAB
- pNIPAm-SDS; pNIPAm diluted with $1,25\ ml$ Milli-Q® water plus $22,8\ \mu l$ of SDS

Table 2.2: The samples are made by starting with a pNIPAm base concentration of $47,9\ mg/ml$. Of each surfactant a dilution is made based on the CMC level. After which four samples are made with an end concentration of $42,57\ mg/ml$. Sample one, pNIPAm; is $1\ ml$ pNIPAm diluted with $1,25\ ml$ Milli-Q® water, sample two, pNIPAm-TRT; pNIPAm diluted with $1,25\ ml$ Milli-Q® water plus $4,7\ \mu l$ of TRT, sample three, pNIPAm-CTAB; pNIPAm diluted with $1,25\ ml$ Milli-Q® water plus $6,7\ \mu l$ of CTAB and sample four, pNIPAm-SDS; pNIPAm diluted with $1,25\ ml$ Milli-Q® water plus $22,8\ \mu l$ of SDS

Surfactant	CMC (mM)
TRT	$0,9$[36]
CTAB	$0,92$[37]
SDS	8[38]

2.4.1. Density

Density is a physical property that is defined as a mass per unit volume and it depends on the mass of the elemental molecules and the amount of molecules per unit volume [39]. The amount of molecules per unit volume can depend on a variety of factors such as pressure and temperature. When temperature increases the molecules gain more energy and separate. This separation means that there will be decrease in the number of molecules per unit volume, hence a lower density. To measure the density a *DMA 5000* from *Anton Paar, Austria* is used. This device uses what is called a Forced Oscillation Method to determine the density of a liquid. The period of the oscillations can be used to calculate the density. Equation (2.6) shows the relation between the period τ and the density.

$$\rho = A\tau^2 - B, \tag{2.6}$$

where τ is the period in seconds, and *A* and *B* are constants to a particular device. These are determined by performing a calibration measurement with air and with water. This experiment is done by using $2\ ml$ of the pNIPAm suspension. At each temperature mentioned in paragraph 2.4 three measurements are taken, which are used to determine the average.

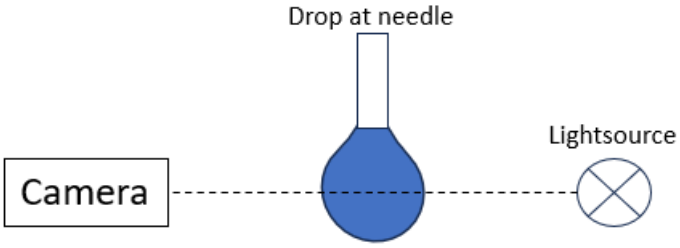

Figure 2.4: Schematic of the pendant drop method, used for measuring the surface tension of pNIPAm, pNIPAm-TRT, pNIPAm-CTAB and pNIPAm-SDS. The light source creates a shadow of the drop which the camera registers. The software calculates the surface tension based on the Young-Laplace equation.

2.4.2. Surface Tension

When there are two or more liquids that do not have the same density and are immiscible, an interface is formed between them. This interface acts like a membrane under tension because of the unbalanced attractive intermolecular forces [40]. Commonly, the surface tension depends on the fluid, the temperature, impurities and the possible presence of chemicals that can change the surface tension, for example surfactants. Surface tension affects the formation of drops, possible satellite drops as well as the spreading of the ink on the substrate. The surface tension is measured by using an *OCA 25 Goniometer* from *DataPhysics Instruments, Germany* accompanied by the software *SCA202 V.5.0.41*, by applying the pendant drop method. A schematic of the method is shown in Figure 2.4 The software used with the OCA 25 Goniometer uses the **Young-Laplace equation** to analyse the drop shape.

$$\Delta p = \gamma\left(\frac{1}{R_1} + \frac{1}{R_2}\right), \tag{2.7}$$

Where Δp is the pressure difference (Pa) over the interface, γ (N/m) the surface tension and R_1 & R_2 (m) the radii of the curvature. At each temperature, 10 measurements are taken, which are used to determine the average.

2.4.3. Viscosity

Viscosity is a property that describes the resistant to shear deformation or flow [41]. The viscosity is temperature depended. When the temperature increases the molecules in the liquid will gain more energy and start to separate which would decrease the cohesive molecular forces and as a result would decrease the viscosity. It is important to know if the viscosity of the ink because this has an influence on the printability of the fluid. To determine the viscosity of the pNIPAm samples, an *Anton Paar, Austria* Rheometer MCR 302 is used with a 25 millimeter diameter parallel plate at a height of $0,145mm$. one measurement consists of a exponential incerase of the shear rate (ramp up) from $0,1$ till 10000 $(1/s)$. This is followed by an exponential decrease in shear rate (ramp down) from 10000 to $0,1$ $(1/s)$. This is done according to the *G. Ovarlez* [42]. These measurements are done at the following temperatures; $20, 30$ and 35°C. At each temperature two measurements consisting of a ramp up and ramp down are conducted, of these measurements the average is taken.

2.4.4. Particle size

Considering the fluid is a suspension of pNIPAm particles it is of importance to determine the size of the particles. In the case of the pNIPAm suspensions it is not pigments but it is the polymer beads that are present. Marin et al. 2018, [43] determined a probability when a suspension could clog the nozzle. This not further examined or studied because it is outside the scope of this thesis. Besides clogging, the size of the particles are important considering the ideal fluid requirements given in table 2.1. To measure the particle size a *Zetasizer Nano ZS* from *Malvern Panalytical,UK* is used, in combination with a ZEN0112 cuvette. To conduct these measurements a volume fraction of 0.25 % of pNIPAm and

Milli-Q® water is used. An average is taken of the 3 measurements conducted at each temperature mentioned in Paragraph 2.4.

2.4.5. Zeta Potential

At the interface of a solid and a liquid a charge is developed. This charge or electric potential at this interface is known as the zeta potential (ζ) (mV). This zeta potential gives an indication how stable the dispersion of the particles on the surface is, if the particles flocculate or disperse evenly over the substrate. The Zeta potential gives an insight on the stability of the pNIPAm beads and the formation of a monolithic layer on the substrate. When the potential is close to $0\ mV$, there is a change that the pNIPAm particles will agglomerate or flocculate. If the zeta potential is high, $\geq \pm 30\ mv$, the particles are dispersed and resist agglomeration. Considering the surfactant used are *non-ionic*, *anionic* or *cationic*, it is important to know if these surfactants have an effect on the stability of the pNIPAm suspension. Table 2.3 shows a general guideline given by Kumar and Dixit, 2017. [44] where it shows when the behaviour of the particles can be considered stable. Typically the range of the zeta potential is between -100 to $+100mV$ [44, 45]. To determine the zeta potential the same equipment as the one used for the particle size measurements is, the *Zetasizer Nano ZS* from *Malvern Panalytical,UK* with a DTS1070 cuvette. To conduct these measurements a volume fraction of 2 % of pNIPAm and Milli-Q® water is used. At the temperatures mentioned in Paragraph 2.4, 10 measurements are taken which are used to determine the average.

Table 2.3: Zeta Potential and stability [44]. The zeta potential gives an insight on the stability of the pNIPAm beads in the suspension. It shows the repulsion between each charged particle. When this is low, there is a change that the particles flucculate. But when the zeta potential is high, it means that the particles are desperesed well enough to avoid aggragation.

Zeta Potential (mV)	Stability Behaviour
0 to ± 5	Flocculation or coagulation
± 10 to ± 30	Incipient instability
± 30 to ± 40	Moderate stability
± 40 to ± 60	Good stability
greater than ± 60	Excellent stability

3

Results & Discussion: Microgel Characterisation

3.1. Microgel Characterisation results

3.1.1. Density

Figure 3.1 shows the density of pNIPAm with various surfactants added. Adding SDS and CTAB has a marginal influence on the overal density of the pNIPAm suspension. However, when adding Triton, the density deviates when the LCST is approached. Of the three surfactants that have been used, TRT is the only one that is of liquid form when it was added to the pNIPAm suspension. The other two are solids. This deviation seen in the graph is consistent with the research done by Szymczyk, Katarzyna & Taraba, Anna. (2016) [46]. Which states that the increase of temperature, results in a volume expansion. This expansion creates more space between the molecules of the surfactant, this leads to a disorganised structure of the molecules. Table 3.1 shows the densities at temperatures 20, 30 and 35°C.

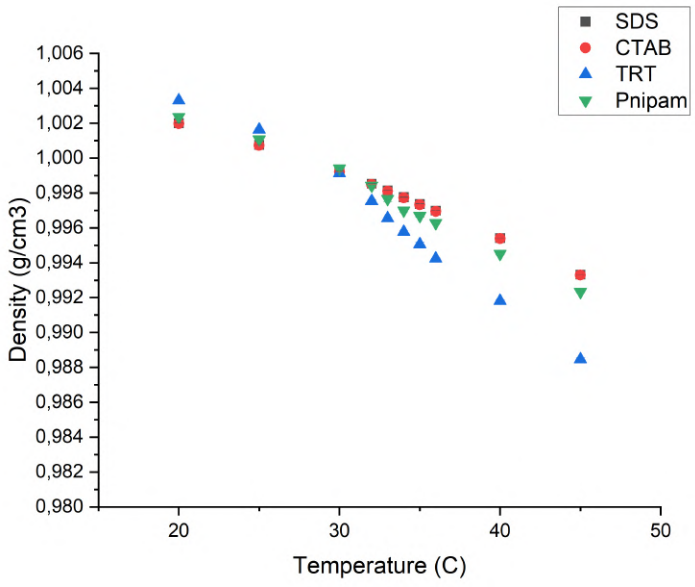

Figure 3.1: This graph shows the average of three measurements the pNIPAm, pNIPAm-TRT, pNIPAm-CTAB and pNIPAm-SDS density ($g/cm3$) vs the temperature (°C). It shows that adding the surfactants SDS and CTAB does not affect the density of pNIPAm compared to the without any added surfactants. However, adding TRT to the suspension does have an effect on the density when the LCST is approached.

Table 3.1: Density ρ (g/cm^3) of pNIPAm, pNIPAm-TRT, pNIPAm-CTAB and pNIPAm-SDS at temperatures 20,30 and 35°C. This table shows that the density decreases when the temperature increases. The standard deviation is determined by three measurements taken at each temperature.

Sample	ρ at 20°C	ρ at 30°C	ρ at 35°C
pNIPAm	$1,00235 \pm 2,16E-5$	$0,99941 \pm 4,34E-5$	$0,99668 \pm 8,71E-5$
pNIPAm-TRT	$1,00331 \pm 7,85E-6$	$0,99913 \pm 3,97E-5$	$0,99505 \pm 1,11E-4$
pNIPAm-CTAB	$1,00197 \pm 1,7E-6$	$0,99921 \pm 2,62E-6$	$0,99733 \pm 4,5E-6$
pNIPAm-SDS	$1,00199 \pm 2,05E-6$	$0,99924 \pm 2,16E-6$	$0,99737 \pm 3,56E-6$

3.1.2. Surface Tension

Surfactants adsorb at the interface, in the case of inkjet printing pNIPAm this is the interface between air and the pNIPAm suspension. The amount of surfactant added is based on the Critical Micelle Concentration (CMC). This is the maximum amount of surfactant that can be added before it has no affect on the surface tension of the pNIPAm. As mentioned in the chapter 2 there are three surfactants that have been used; Triton X-114 (TRT), Sodium Dodecyl Sulphate (SDS) and Hexadecyltrimethylammonium bromide (CTAB). The methods described in Chapter 2.3.4 is used. Figure 3.2 shows the surface tension measured at various temperatures. The pNIPAm without any added surfactant has an average surface tension of $67,44\ mN/m$ at 20°C. Where pNIPAm-SDS is $42,7\ mN/m$, pNIPAm-CTAB is $41,55\ mN/m$ and pNIPAm-TRT is $38,39\ mN/m$. Table 3.2 shows the surface tension at at temperatures 20, 30 and 35°C. The surface tension decreases when the temperature increases.

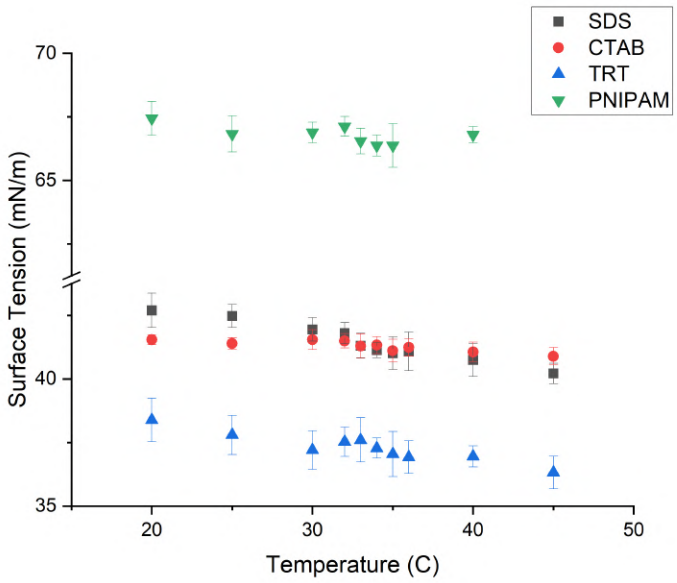

Figure 3.2: The graph shows the average surface tension of ten measurements of pNIPAm, pNIPAm-TRT, pNIPAm-CTAB and pNIPAm-SDS vs Temperature (°C). It can be seen that the surface tension decreases when the surfactants are added to the pNIPAm suspension. Also, that it decreases when the temperature increases. Of the three surfactants used Triton X-114 lowers the surface tension the most. The standard deviation is determined by three measurements taken at each temperature.

Table 3.2: Surface Tension γ (mN/m) of pNIPAm, pNIPAm-TRT, pNIPAm-CTAB and pNIPAm-SDS at temperatures 20,30 and 35°C. It can been seen that the surface tension for all samples decrease when the temperature increases. Of the three surfactants Triton X-114 lowers the surface tension the most, from $67,44$ till $38,4\ mN/m$.

Sample	γ at 20°C	γ at 30°C	γ at 35°C
pNIPAm	$67,44 \pm 0,67$	$66,88 \pm 0,41$	$66,37 \pm 0,85$
pNIPAm-TRT	$38,4 \pm 0,86$	$37,20 \pm 0,76$	$37,04 \pm 0,89$
pNIPAm-CTAB	$41.55 \pm 0,20$	$41,55 \pm 0,39$	$41,12 \pm 0,44$
pNIPAm-SDS	$42,70 \pm 0,68$	$41,95 \pm 0,46$	$41,01 \pm 0,64$

3.1.3. Viscosity

The assumption that is made in chapter 2 is that the pNIPAm microgel behaves as a Newtonian fluid when the Shear Rate is of the 10^5 order of magnitude. To validate this assumption various rheological experiments have been conducted using the equipment and method mentioned in chapter 2.3.4. Figure 3.3 shows the Shear stress vs Shear rate. This shows that when the temperature is increased the shear stress decreases. While Figure 3.4 shows the Viscosity vs Shear rate for different temperatures. It shows that for all samples the viscosity decreases when the temperature is increased.

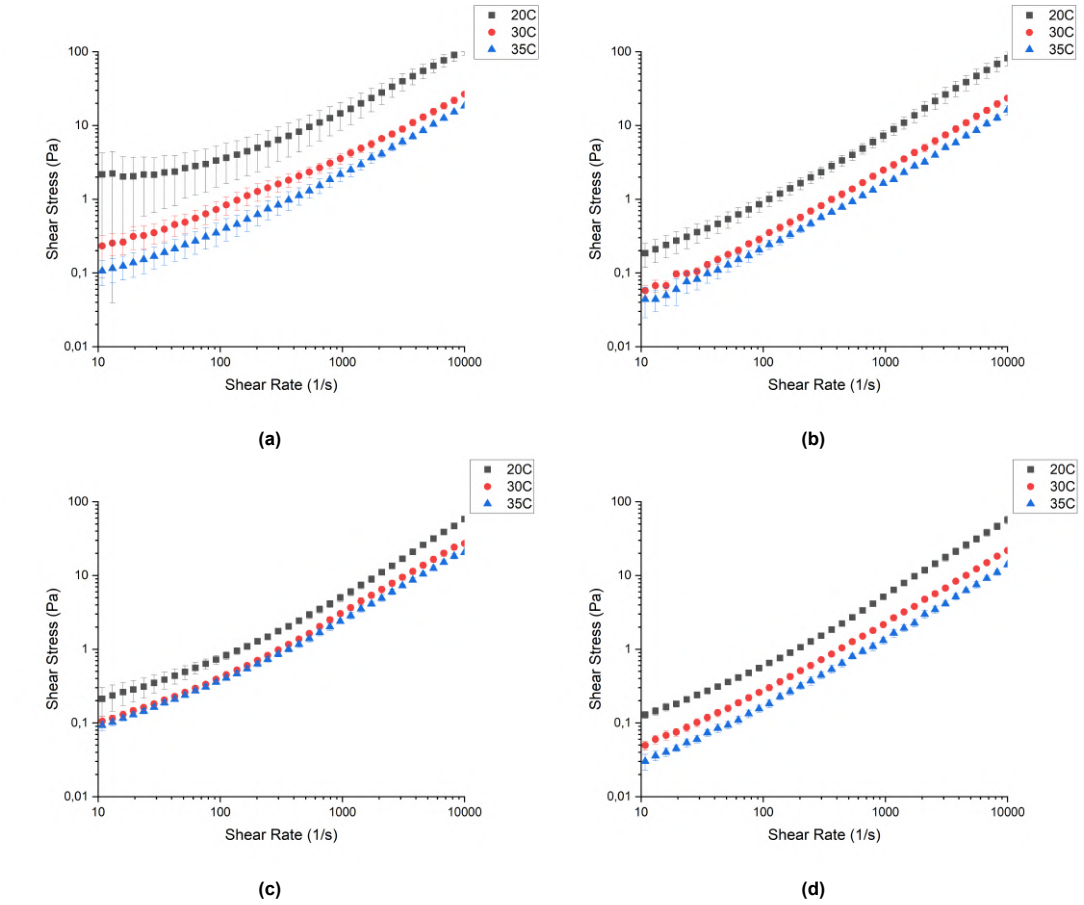

Figure 3.3: Shear Stress vs Shear Rate of pNIPAm (*a*), pNIPAm-TRT (*b*), pNIPAm-CTAB (*c*) and pNIPAm-SDS (*d*) at temperatures 20,30 and 35°C. As can be seen in *a,b,c* and *d* the measured shear stress lowers when the temperature decreases. The standard deviation shown is determent by two measurements.

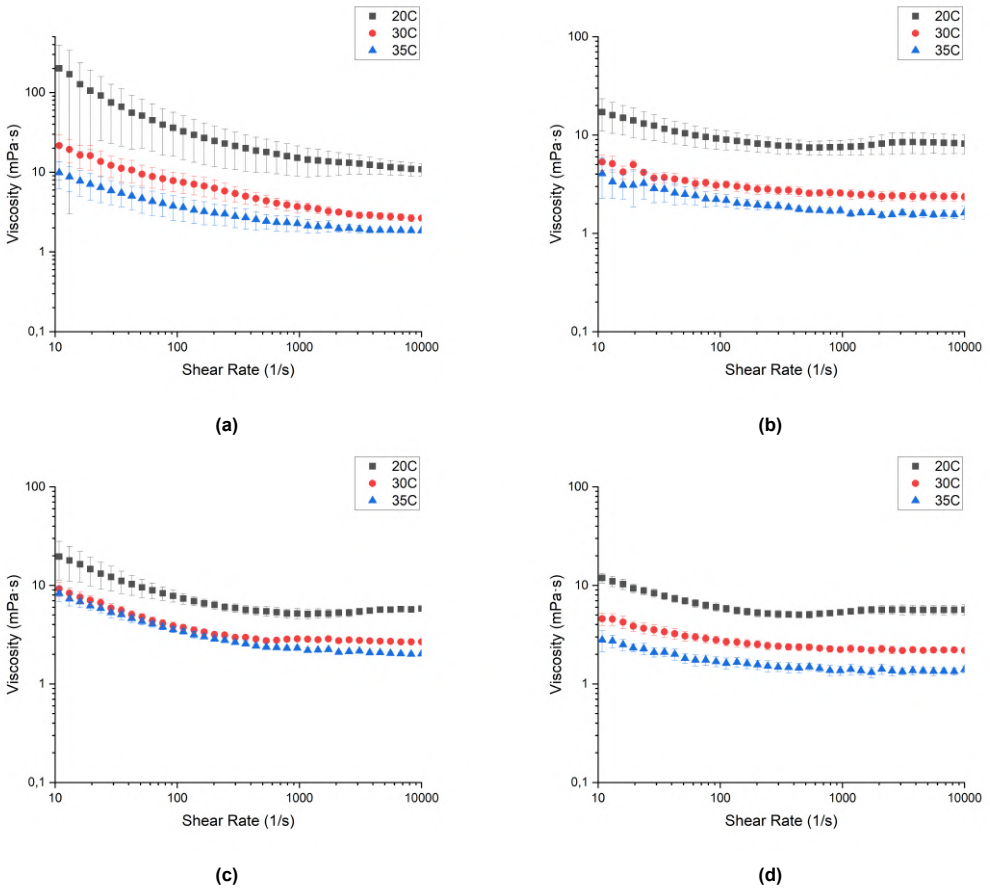

Figure 3.4: Viscosity vs Shear Rate of pNIPAm (*a*), pNIPAm-TRT (*b*), pNIPAm-CTAB (*c*) and pNIPAm-SDS (*d*) at temperatures 20,30 and 35°C. It shows in *a,b,c* and *d* that when the temperature increases the viscosity deceases. The standard deviation shown is determent by two measurements.

Figure 3.5 compares pNIPAm and the various surfactants added. In figure 3.5a, 3.5c and 3.5e, the shear stress vs the shear rate is compared. It shows that at high shear rates in the order of 10000 $1/s$ the surfactants have little to no influence on the measured shear stress. The same can be said about Figures 3.5b, 3.5d and 3.5f, which compares the viscosity vs shear rate of pNIPAm, pNIPAm-TRT, pNIPAm-CTAB and pNIPAm-SDS. The added surfactants play minimal to no role when it comes to the measured viscosity. Only at a temperature of 20°C there is a notable difference in the viscosity. For pNIPAm, $10,90\ mPa \cdot s$ and for pNIPAM-CTAB, $5,68\ mPa \cdot s$. However, if there is a relation between the surface tension and the viscosity has not been investigated. The pNIPAm suspensions show shear thinning behavior at low shear rates up to $300\ 1/s$, the viscosity decreases as the shear rate increases seen in Figure3.5. At higher shear rates of 1000 till $10000\ 1/s$ the viscosity and shear stress are constant. Therefore, depositing pNIPAm with an inkjet printer it can be assumed to be Newtonian fluid. Based on the requirements given in Table 2.1 the best suited temperature to print would be at 20°C. Table 3.3 shows the measured viscosity at 20, 30 and 35 °C and at a shear rate of $10000\ 1/s$. At low shear rate there is a noticeable difference between the measured viscosity and shear stress, when pNIPAm is compared to pNIPAm with the added surfactants. A cause of this deviation can be due to the fact that the surface tension of the pNIPAm without any added surfactant is higher and therefore can impact the measured torque [47]. Which as consequence affects the measured shear stress and viscosity.

Table 3.3: Measured viscosity of pNIPAm, pNIPAm-SDS, pNIPAm-TRT and pNIPAm-CTAB at a shear rate of $10000\ 1/s$ at 20, 30 and 35°C. At 30 and 35°C, the surfactants have little to no influence on the viscosity. However, at 20°C, there is a noticable difference in the viscosity. It is however not investigated if the surface tension has an relation with the viscosity.

Sample	Viscosity ($mPa \cdot s$) 20°C	Viscosity ($mPa \cdot s$) 30°C	Viscosity ($mPa \cdot s$) 35°C
pNIPAm	$10,90 \pm 1,92$	$2,65 \pm 0,19$	$1,184 \pm 0,03$
pNIPAm-SDS	$8,19 \pm 1,83$	$2,35 \pm 0,22$	$1,62 \pm 0,25$
pNIPAm-TRT	$5,81 \pm 0,24$	$2,67 \pm 0,06$	$2,02 \pm 0,05$
pNIPAm-CTAB	$5,68 \pm 0,70$	$2,18 \pm 0,11$	$1,40 \pm 0,11$

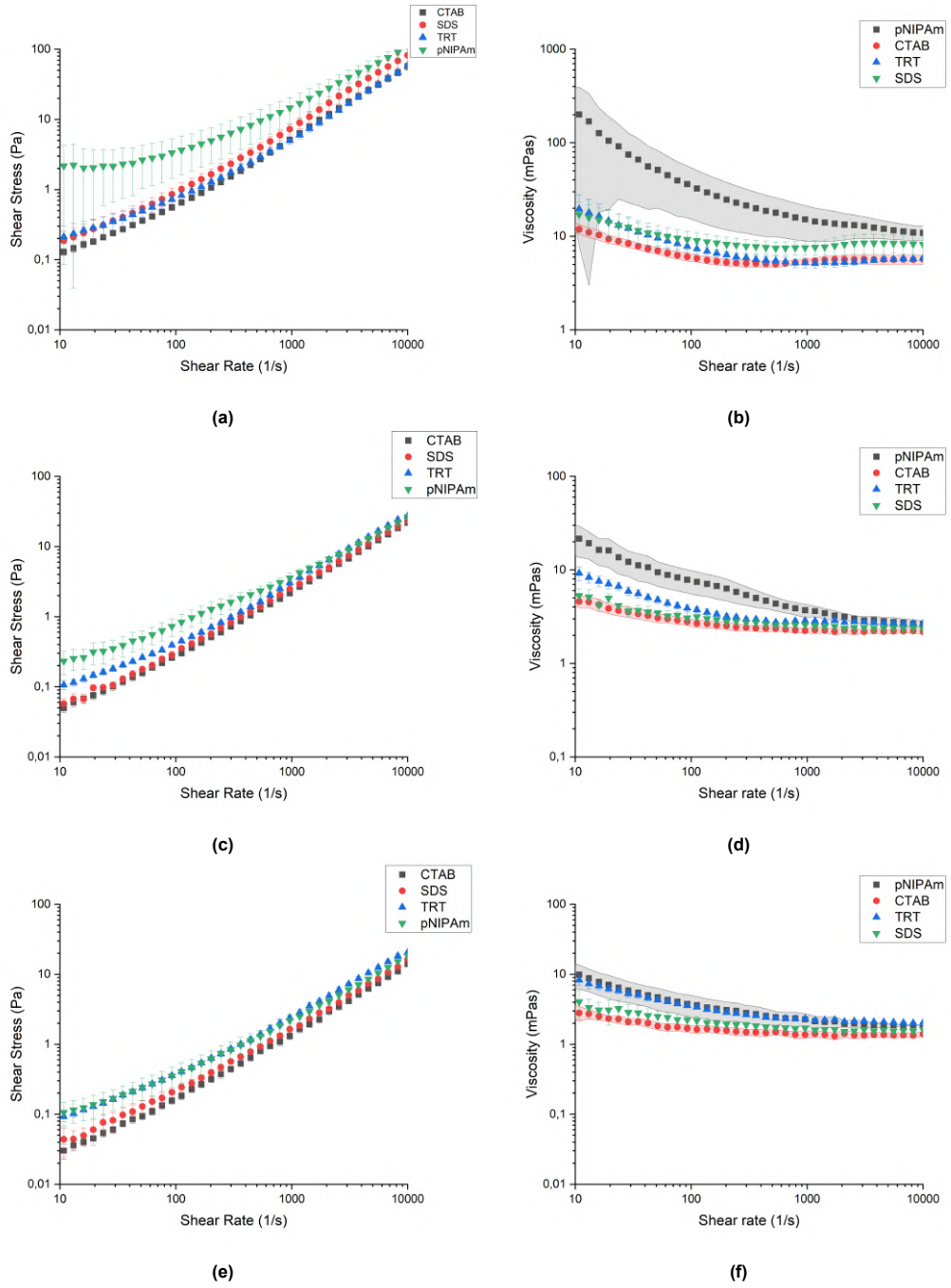

Figure 3.5: *a*, *c* and *e* shows the Shear stress vs Shear rate at 20,30 and 35°C of pNIPAm, pNIPAm-TRT, pNIPAm-CTAB and pNIPAm-SDS. At high shear rate the added surfactants have little influence on the measured shear stress. Figures *b*, *d* and *f* compares the Viscosity vs Shear rate at 20, 30 and 35°C for pNIPAm, pNIPAm-TRT, pNIPAm-CTAB and pNIPAm-SDS. The added surfactants have no meaningful influence on the viscosity at a shear rate of $10000\ 1/s$. The values shown in the graph represent the average taken from two measurements.

3.1.4. Particle size

The pNIPAm particles have the ability to change their size depending on the temperature they are exposed to. The advise given by table 2.1 shows that the particles should be sub micron. Figure 3.6 presents the change of pNIPAm particles size with respect to temperature. The initial size at 20°C for all the studied samples are in the range of $924,33\ nm$ for pNIPAm, to $1051\ nm$ for pNIPAm-CTAB. Increasing the temperature leads to a decrease of the particle size reaching a minimum of $411,43\ nm$ for pNIPAm to and for pNIPAm-CTAB $409,53\ nm$. This decrease is as expected and found in literature [48]. The surfactants do not have an influence on the particle size of the pNIPAm beads. Table 3.4 shows the particle size of each sample at 20°C, 30°C, 35°C and 45°C.

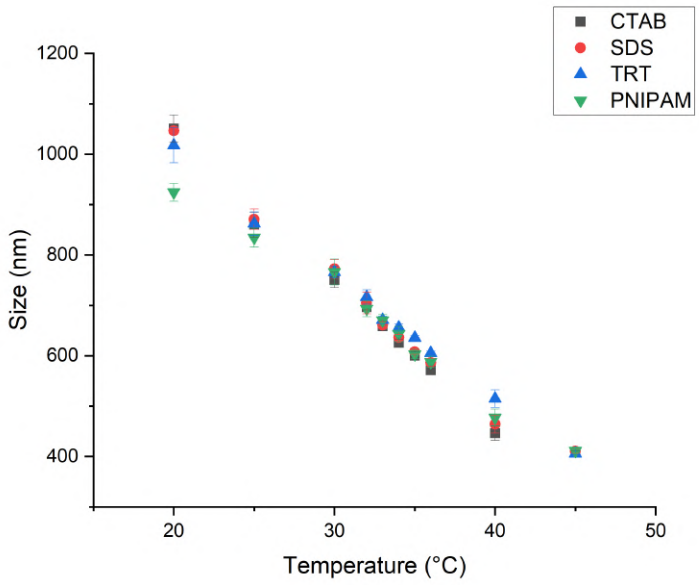

Figure 3.6: Particles size (nm) of pNIPAm, pNIPAm-TRT, pNIPAm-CTAB and pNIPAm-SDS vs Temperature (°C). Adding surfactants have minimal influence one the size of the pNIPAm particles. Each data point in the graph is an average of three measurements. As the literature suggests, the pNIPAm particles decrease in size when the temperature is increases.

Table 3.4: Particles size nm of pNIPAm, pNIPAm-TRT, pNIPAm-CTAB and pNIPAm-SDS at temperatures 20,30, 35 and 45°C.

Sample	at 20°C	at 30°C	at 35°C	at 45°C
pNIPAm	$924,33 \pm 17,52$	$766,23 \pm 25,80$	$603,133 \pm 0,03$	$411,43 \pm 3,15$
pNIPAm-SDS	$1046,67 \pm 6,85$	$772,4 \pm 18,32$	$607,93 \pm 4,78$	$406,03 \pm 2,50$
pNIPAm-TRT	$1017,67 \pm 34,66$	$766,23 \pm 12,01$	$635,37 \pm 4,65$	$411,43 \pm 3,15$
pNIPAm-CTAB	1051 ± 27	$750,33 \pm 15,21$	$600,37 \pm 7,34$	$409,53 \pm 1,11$

3.1.5. Zeta Potential

Three surfactants have been used to lower the surface tension of the pNIPAm suspension, the three surfactants are Triton X-114 (TRT), *non-ionic*, *Sigma-Aldrich laboratory grade*, Sodium Dodecyl Sulphate (SDS), *anionic*, *Sigma Aldrich* $\geq 99,0\%$ and Hexadecyltrimethylammonium bromide (CTAB), *cationic Sigma Aldrich* $\geq 98\%$. Adding the surfactants have an effect on the Zeta potential seen in Table 3.5. It shows that the anionic surfactant SDS lowers the zeta potential the most while the cationic surfactant CTAB lowers the zeta potential the least. The non-ionic surfactant TRT is in between the two other surfactants.This change in zetapotential is due to the deprotonation of acrylic acid which is present in the pNIPAm suspension. But according to Table 2.3 all samples show incipient instability. This means that there is a chance that the particles can agglomerate and/o flocculate which can cause nozzle clogging. The graph shown in Appendix A FigureA.1 represent the overall trend regarding the zeta potential vs temperature.

Table 3.5: The Measured Zeta potantial at 45°C. it shows that adding surfactants lowers the overall zeta potential. Of the three surfactants the anionic surfactant SDS lowers the zeta potential the most. While the non-ionic surfactant TRT is in between SDS and CTAB the cationic surfactant.

Sample	Zeta Potential (mV) at 45°C
pNIPAm	$-25,2 \pm 1,21$
pNIPAm-TRT	$-26,3 \pm 0,68$
pNIPAm-CTAB	$-26,1 \pm 0,43$
pNIPAm-SDS	$-26,7 \pm 0,05$

3.1.6. Which surfactant?

Based on the results of this chapter it is chosen to use Triton X-114 as the surfactants. Each of the suggested surfactants have minimal influence on the viscosity measured at a shear rate of $10000\ 1/s$ as seen in paragraph 3.1.3. This can also be said about the particle size and density. As expected the biggest impact each surfactant has is on the surface tension. Both SDS and CTAB reduce the surface tension significantly compared the original pNIPAm suspension, $67,44\ mN/m$ to $42,70\ mN/m$ and $41,55\ mN/m$ respectively. But TRT reduces the surface tension the most, from $67,44\ mN/m$ to $38,39\ mN/m$ at 20°C. This is still higher than the ideal fluid requirements given by ***Fuijifilm*** for their ***Dimatix*** cartridge which is between 28 and $32\ mN/m$. Hence, the surfactant that will be used for testing the printability of pNIPAm is Triton X-114.

3.1.7. Ohnesorge, Reynolds and Weber Number

As mentioned in chapter 2 the Ohnesorge gives the stability of the drop and it estimates if the pNIPAm would be able to produce a drop. To determine the velocity which is needed to calculate the Reynolds and Weber number Equation 2.7 is used. Table 3.6 shows all the characteristics of the sample pNIPAm-TRT, this table only includes Triton X-114 because that is the surfactant chosen to be used for further experiments. Figure 3.7 shows Ohnesorge number corresponding to the temperatures 20(blue), 30(green) and 35°C(red). It shows that using the calculated velocity it will not be able to produce drops, because there is insufficient energy. As seen in Table 3.7 the Weber number is 4. The criteria given by ***Derby,2010***[27] says the Weber number should be higher than 4.

Table 3.6: The measured characteristics of pNIPAm-Triton X114 at shear rate of $10000\ 1/s$ and temperatures 20,30 and 35°C.

Parameter	at 20°C	at 30°C	at 35°C
Density (g/cm^3)	$1,00331$	$0,99913$	$0,99505$
Surface Tension (mN/m)	$38,40$	$37,20$	$37,04$
Viscosity ($mPa \cdot s$)	$5,81$	$2,67$	$2,02$
Nozzle size (μm)	$23,25$	$23,25$	$23,25$
Minimum Velocity (m/s)	$2,57$	2.53	2.53
Particle size (nm)	$1017,67 \pm 34,66$	$766,23 \pm 12,01$	$635,37 \pm 4,65$

Table 3.7: The Reynolds, Weber and Ohnesorge Number for pNIPAm-TRT at a temperatures of 20, 30 and 35°C. Given that the requirement is We ≥ 4), indicates that there will be no drop ejected due to the lack of kinetic energy.

	at 20°C	at 30°C	at 35°C
Re	$10,28$	$22,02$	$28,98$
We	$3,98$	$4,00$	$4,00$
Oh	$0,194$	$0,091$	$0,069$

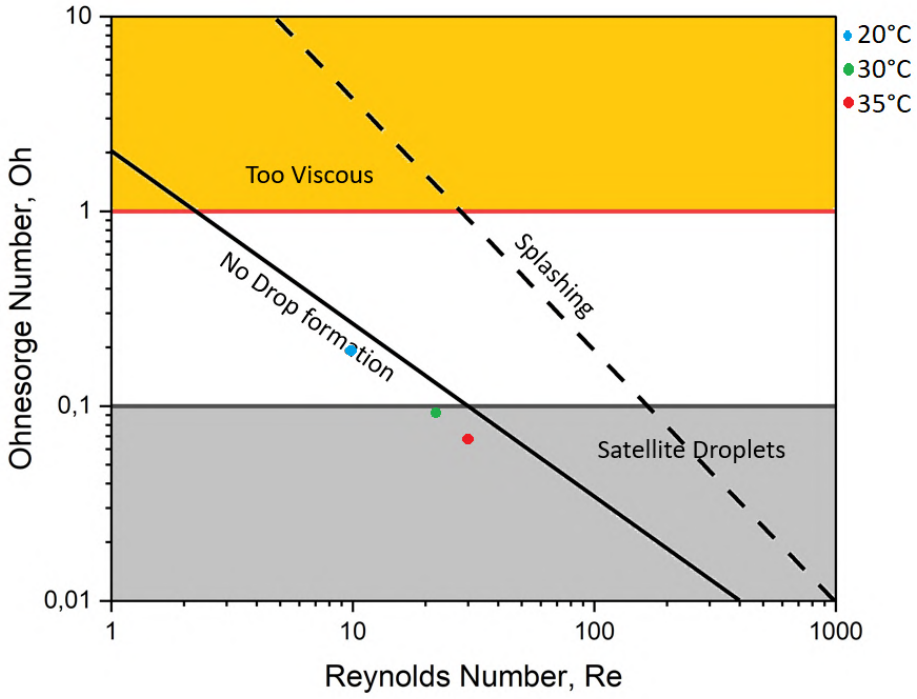

Figure 3.7: Diagram of the operating regime for stable drops. The dots blue (20°C), green (30°C) and red (35°C) show that using the calculated velocity will not result in pNIPAm-TRT drop formation.

Results & Discussion: Printing

3.2. Printing

Chapter 3 concluded that the surfactant that will be used onwards to investigate if it is possible to deposit pNIPAm on glass substrates is Triton X-114 . As previously mentioned the printer that will be used is a *LP50 PIXDRO* inkjet printer as seen in figure 2.1. Besides the chosen surfactant, the temperature range that will be investigated is between 30 and 35°C. This chapter will also investigate if the deposited pNIPAm is able to form a monolithic layer on the substrate by the use of an SEM. The size of the print is decided to be a diameter of $3\ mm$. This is due to the fact that the Organ on Chip (OoC) that inspired this research has an available surface of $3\ mm$. It is possible to increase the Dots-Per-Inch or DPI. Just like the name suggests this means how many dots are deposited per inch during printing. The higher the DPI, the better the resolution. The DPI's that are chosen were 500, 1500, 2000 and 4000. These were chosen because at 500 DPI the deposited drops would, according to the software of the *LP50 PIXDRO* create individual drops. While the other DPI's would create the illusion of one single drop of $3\ mm$ diameter. Thus better comparable to spincoated samples.

3.2.1. Print settings

Figure 3.8a shows a schematic of a waveform that is used for inkjet printing. Various settings can be changed when it comes to the waveform. The applied voltage and its amplitude affects the nozzle chamber. The pulse width determines the period this voltage is applied to the nozzle chamber. While the pulse spacing determines the pause that is between pulses. The applied voltage has an influence on the drop speed and the possibility of producing satellite drops. Satellite drops is a phenomenon where there are one or multiple small drops after the ”main” ink drop. This can influence the overall quality of the print. The pulse width is used to optimize the drop speed for the voltage that has been used. The first step that has been taken was using the default settings of the inkjet printer. These defaults settings of the printer are;

- the Waveform; Voltage of $26mV$, Pulse width of $2,2\mu s$ and a pulse space of $4,5\ \mu s$
- the number of iterations; means how many times the printer will print on the same figure on the same spot, default is one iteration
- print direction; the *LP50* allows the print-head to move or the substrate-bed, the default setting is that the substrate-bed moves and the printhead stays still
- substrate-bed temperature; it is possible to heat the substrate-bed, the default setting is that the bed heating is turned off
- printhead temperature; this is the temperature that heats the ink in the cartridge, default setting this is turned off

There are more settings but this requires further research. The settings that are used to deposit pNIPAm-TRT on a golden substrate are;

- the Waveform; two pulses where the first pulse is of Voltage $38.8mV$, Pulse width of $2,2\mu s$ and a pulse space of $4,5\ \mu s$. While the second pulse has a Voltage of $10.0mV$, Pulse width of $3,2\mu s$ and a pulse space of $4,5\ \mu s$ seen in Figure 3.8b. This waveform is found by trial and error by visualy looking at the drop seen in Figure Figure3.8c and the corresponding prints. These trial prints can be seen in Appendix A, (FigureA.8, A.9 and A.10).
- the number of iterations; This is kept at one unless it is mentioned.
- print direction; The default settings is kept, meaning the substrate bed moves while the printhead stayed still. This is to keep the amount of variables to a minimum
- substrate-bed temperature; this is kept off, just like the print direction, this is not changed to keep the variables to a minimum

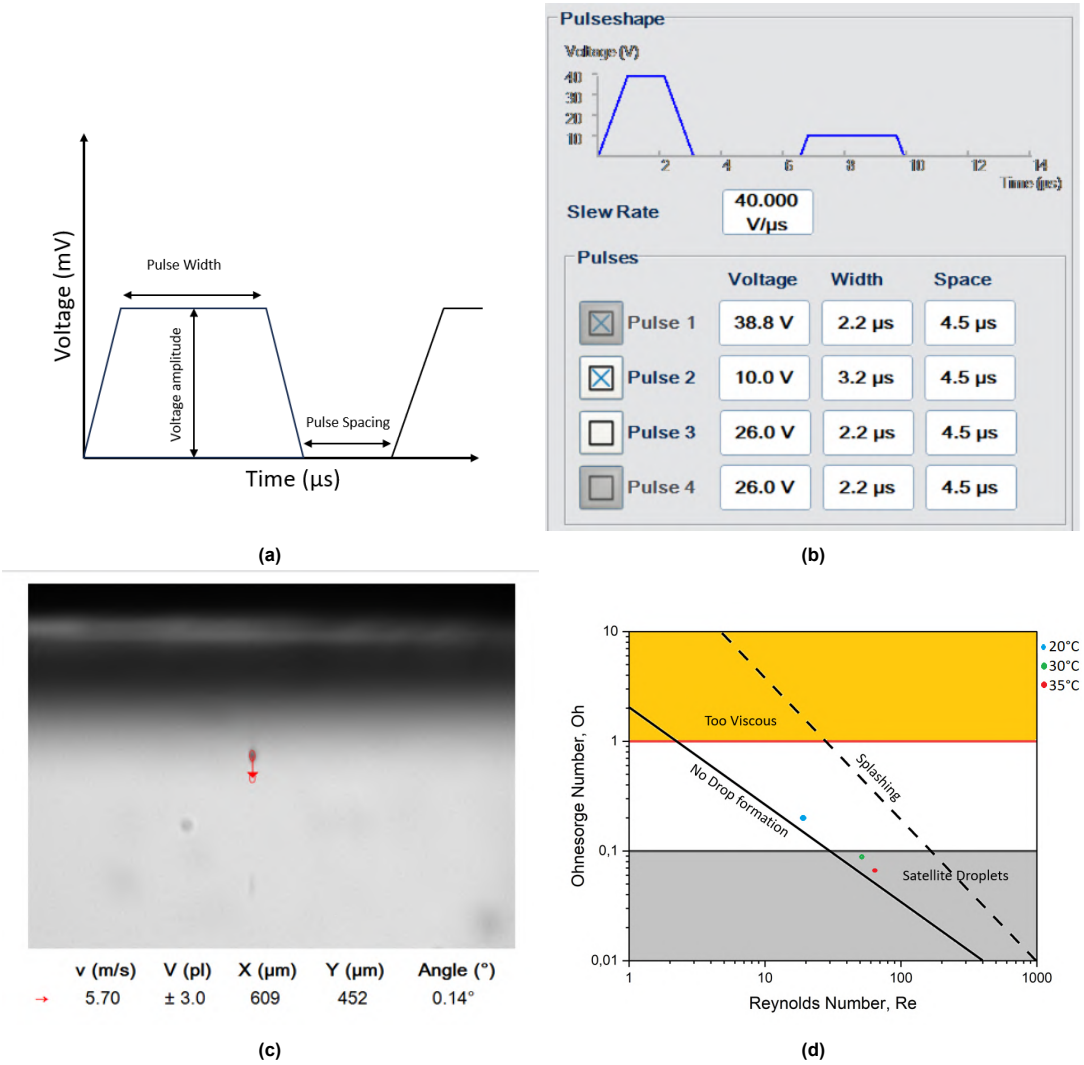

Figure 3.8: (*a*) shows a schematic of a Waveform for inkjet printing. (*b*) shows the waveform that is used to jet the pNIPAm. (*c*) shows the drop velocity and drop volume. The arrow represents the angle in which the drop is falling. Ideally this angly should be $0°$because that means the the drop jets straight. (*d*) shows the dots blue ($20°$C), green ($30°$C) and red ($35°$C) using the measured velocity. Of theses three temperatures, the $20°$C, is the only temperature what is in the printable area. While the other two, $30°$C and $35°$C are in the regime where satellite drops can be formed.

- printhead temperature; this is set to a temperature of 33°C. This is chosen because there was no jetting at 20°C. While drops started to form at 33°C

Using the dedicated *LP50* software it is possible to determine the size and velocity of the drop. The velocity of a drop at 33°C print-head temperature is $5,70\ m/s$ and it has a volume of $3,0\ pl$. The velocity given by the software is higher than the minimum required velocity that is needed to overcome the surface tension determined by using equation 2.7, which is $2,98\ m/s$. This changes the actual Reynolds and Weber number which can be seen in Table 3.8. The We is greater than 4, thus passed the No Drop Formation because insufficient kinetic energy. Comparing Figure 3.8d with Figure3.7 shows that with the new velocity moves the printing region to the right and passed the No Drop Formation barrier. However, of the three temperatures, 20°C is the most suitable option according to this graph. But, at this temperature there was no pNIPAm jetting out of the cartridge. This could be caused by the fact that the pNIPAm particles are $1017,67\ nm$ at this temperature. This is larger than the ideal particle size given in Table 2.1. Hence, it is needed to increase the temperature of the cartridge, so that the particles shrink to sub micron.

Table 3.8: The Reynolds, Weber and Ohnesorge Number at a temperature of 20,30 and 35°C calculated with the new measured velocity of $5,70\ m/s$.

	at 20°C	at 30°C	at 35°C
Re	$22,88$	$49,59$	$65,28$
We	$19,73$	$20,29$	$20,29$
Oh	$0,194$	$0,091$	$0,069$

3.2.2. Print results

500 DPI

The printed result of the 500 DPI can be seen in figure 3.9. Figure 3.9a shows that it is possible to form an evenly distributed print with pNIPAm. It is however not optimal. There are dark spots which can be seen in the lower part of Figure 3.9a. This likely caused by not using the optimal waveform and inkjet printer settings. Considering the print direction is from bottom to top, it could be that during the brief period of the cartridge moving to the bottom, more particles agglomerate in the nozzle. As a result it jets more particles compared to the others. This requires more research in finding the optimal inkjet printer settings. Using the SEM, it shows that there is a monolithic layer of pNIPAm and this is consistent within each individual drop. This can be seen in Figures 3.9b, 3.9c and 3.9d. The size of and spacing between each drop can be seen in Figure3.9e. Each drop is roughly 22 to 23 μm in diameter and the distance between each drop is between 26 and 30 μm. The shaded roster in Figure 3.9a is caused by the microscope and is not present on the actual print.

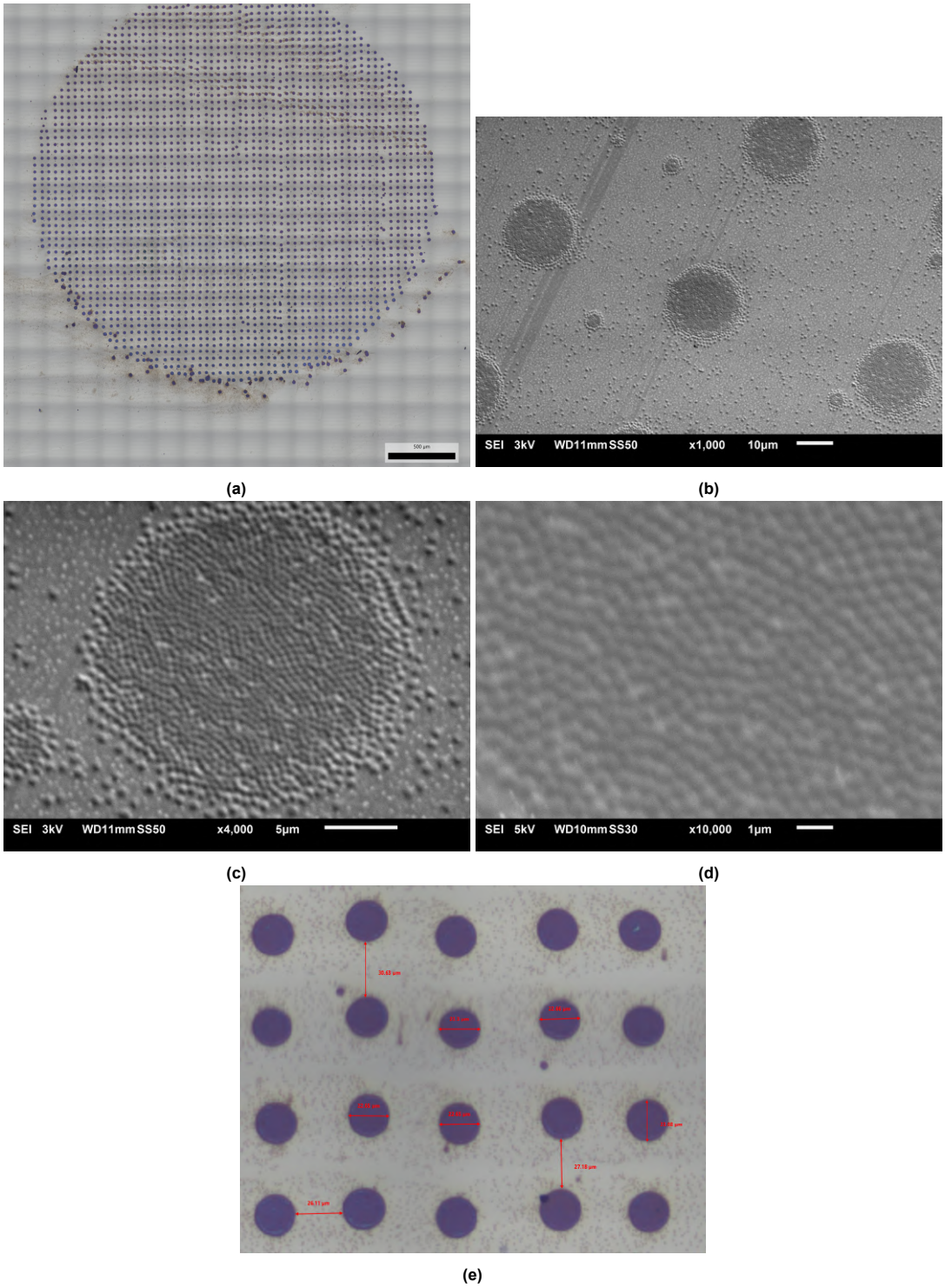

Figure 3.9: (*a*)Optical microscope image showing a print of 500 DPI. The shaded roster is caused by the microscope and is not present on the actual print. (*b*) SEM image of a 500 DPI print at 1000x magnification, (*c*) SEM image 4000x magnification, (*d*) SEM image 10000x magnification of a printed pNIPAm-TRT sample at a DPI of 500 and (*e*) shows the drop size and spacing between each drop.

1500 DPI

The next print is one of 1500 DPI. Figure 3.10 shows a picture taken from the NanoRo microscope of the printed pNIPAm and SEM pictures at various magnifications. The bad quality of the print is quite noticeable in figure 3.10a. Even though the simulated print showed that the drops would fuse. It is actually not the case. This could be caused by the fact that the pNIPAm is not optimised as a jettable ink as seen in chapter 3. Another cause of this could be that the used waveform, is not optimal. The SEM pictures shown in figure 3.10b, 3.10c and 3.10d shows that where the drops did fuse together a monolithic layer is formed. Under SEM the monolithic layer of the beads formed in the gold/white spot in the middle of the print (Figure3.10a) was observed and it was noticed that they were more densely packed compared to the blue parts (FigureA.7,appendix). This spot is formed after following the steps given in paragraph 2.3.2. Specifically during the step between rinsing it with Milli-Q® water and drying it overnight. It was noticed that spot would form where the residual water stayed after rinsing.

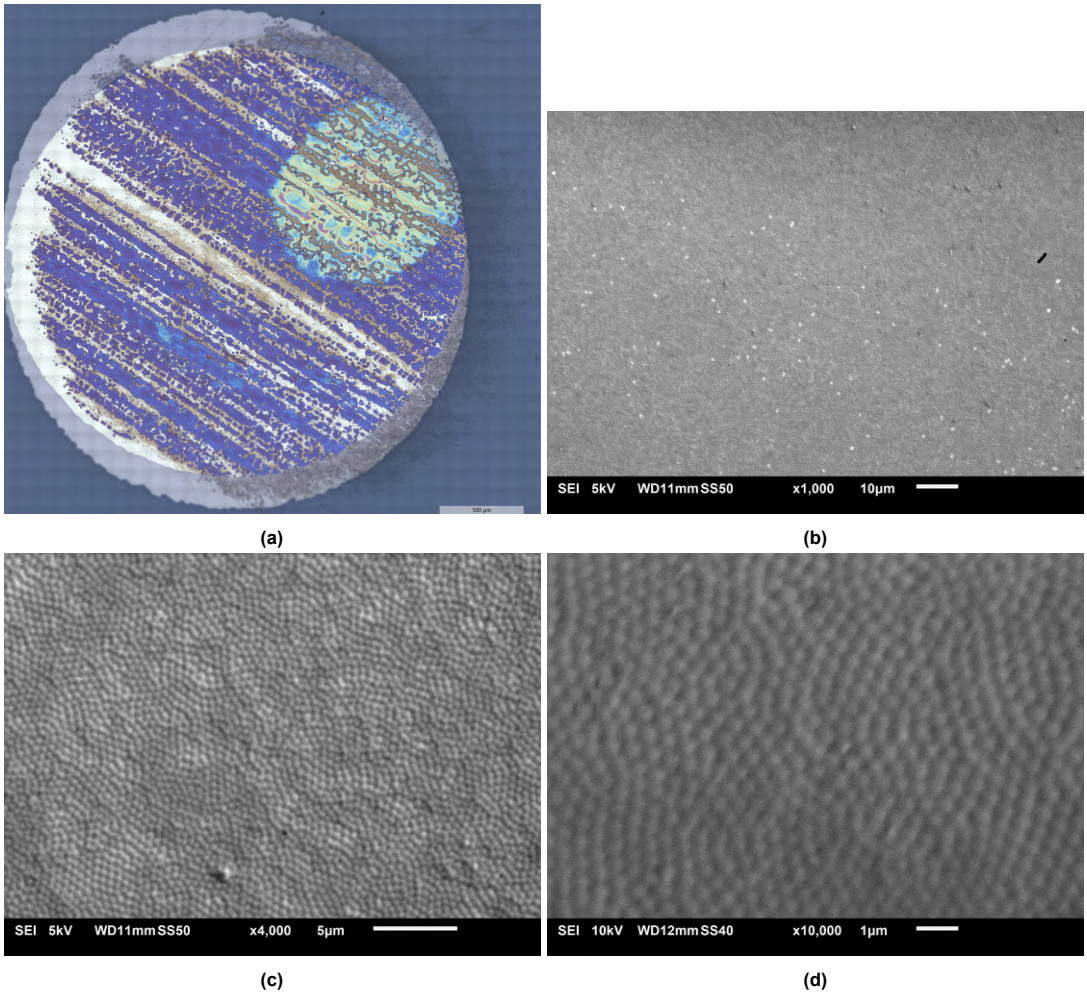

Figure 3.10: *a)* Optical microscope image showing a print of 1500 DPI, (*b*), (*c*) and (*d*) are SEM images at 1000x, 4000x and 10000x magnification of a printed pNIPAm-TRT sample at a DPI of 1500. The SEM pictures are taken in the blue area of the print. It shows that a monolithic layer is formed of the pNIPAm particles.

2000 DPI

As seen in Figure 3.10a, it is still possible to see the golden substrate layer. This is not ideal, because the spectrometer would measure not only a pNIPAm layer but also the gold layer. Thus, an incear in the DPI to 2000 is a necessity. There are still spots where the substrate is visible. Again a gold/white drop is formed where a residual water drop was located before the sample went into the oven. There are still some areas that are not covered by the pNIPAm. This is caused by the fact that the printer settings and the pNIPAm ink are not optimised. Looking at the SEM pictures in figure 3.11b,3.11c and 3.11b, shows that a monolithic layer is formed.

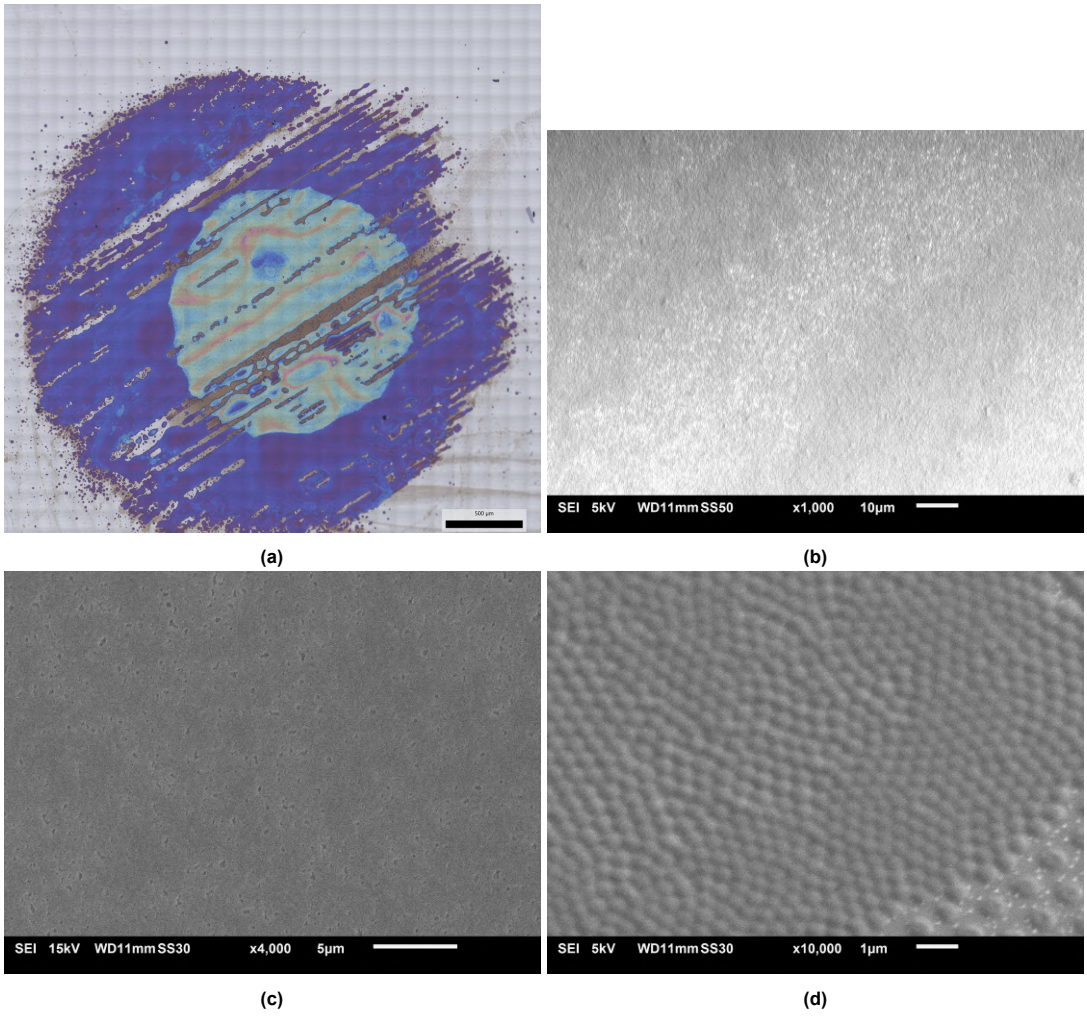

Figure 3.11: *a)* Optical microscope image showing a print of 2000 DPI, (*b*), (*c*) and (*d*) are SEM images at 1000x, 4000x and 10000x magnification of a printed pNIPAm-TRT sample at a DPI of 2000. All the images show that a monolithic layer of pNIPAm particles is achieved.

4000 DPI

Increasing the DPI further from 2000 to 4000, results in a printed sample shown in figure 3.12a. It shows that the drops form visually one cohesive drop. It has to be mentioned that there are still some drops that splashed outside the intended print area. This can be caused by the fact that the Oh number is $0,105$ which is on the border where satellite drops are formed. Looking at figure 3.12b, 3.12c and 3.12d. It clearly shows that a monolithic layer is formed by the pNIPAm particles.

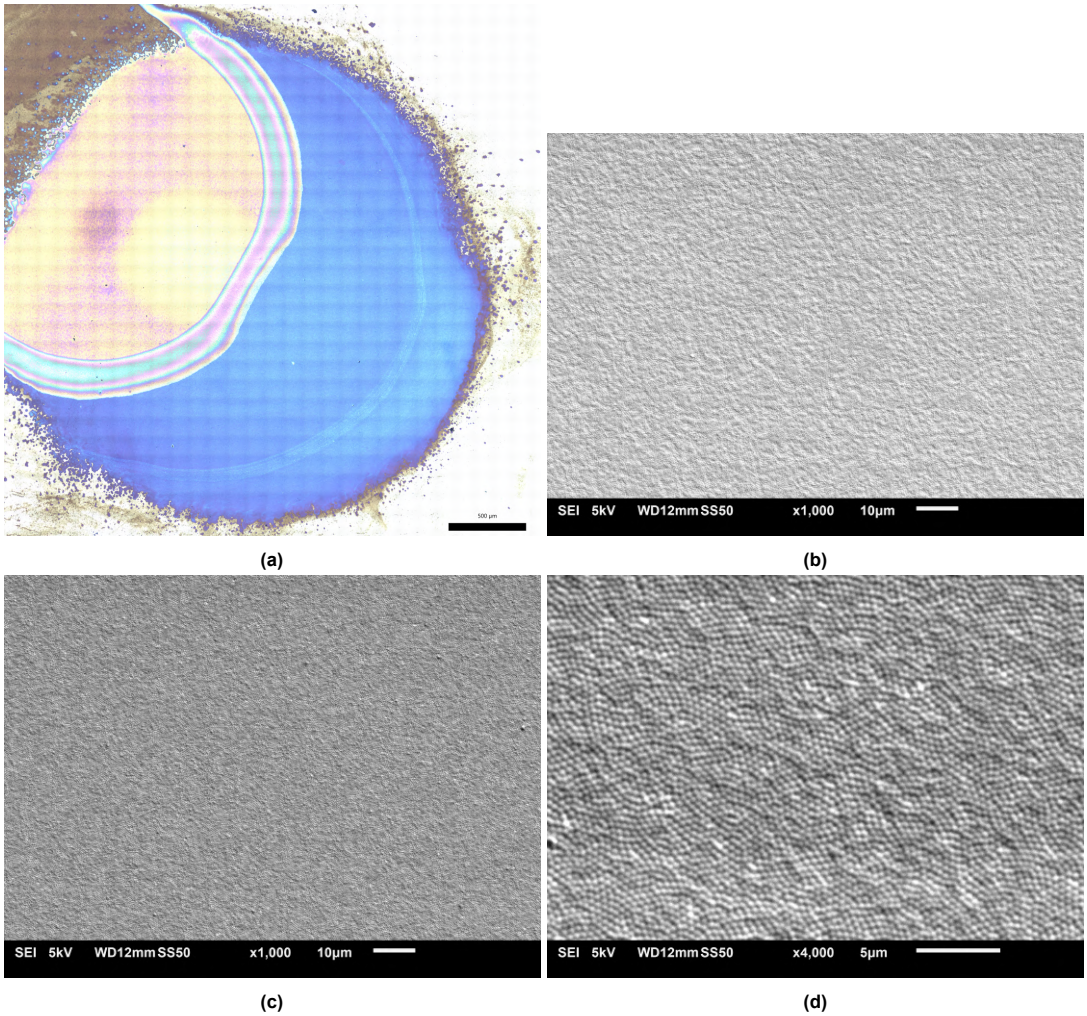

Figure 3.12: *a)* Optical microscope image showing a print of 4000 DPI, (*b*), (*c*) and (*d*) are SEM images at 1000x, 1000x and 40000x magnification of a printed pNIPAm-TRT sample at a DPI of 2000. All the images show that a monolithic layer of pNIPAm particles is achieved.

1500 DPI 2 iterations

Figure 3.10a shows that the substrate is not completely covered when one iteration of printing is used. To see if this could be prevented, it was chosen to print twice over the same spot or two iterations. Between each iteration the sample was rinsed to remove any loose pNIPAm particles. The result can be seen in figure 3.13. It shows that there are less gaps. The substrate is less visible and the drop looks almost like one cohesive drop. The biggest concern using two iterations was that it would not create a monolithic layer with the pNIPAm particles. Figure 3.13b clearly shows two separate prints on top of each other. The vertical strips are from one print and the darker spots on top of those are the second print. At higher magnification in figure 3.13c it seems like a monolithic layer is formed. However, zooming in further, figure 3.13d shows that there is a hill like landscape, which could indicate a multi layer of pNIPAm particles.

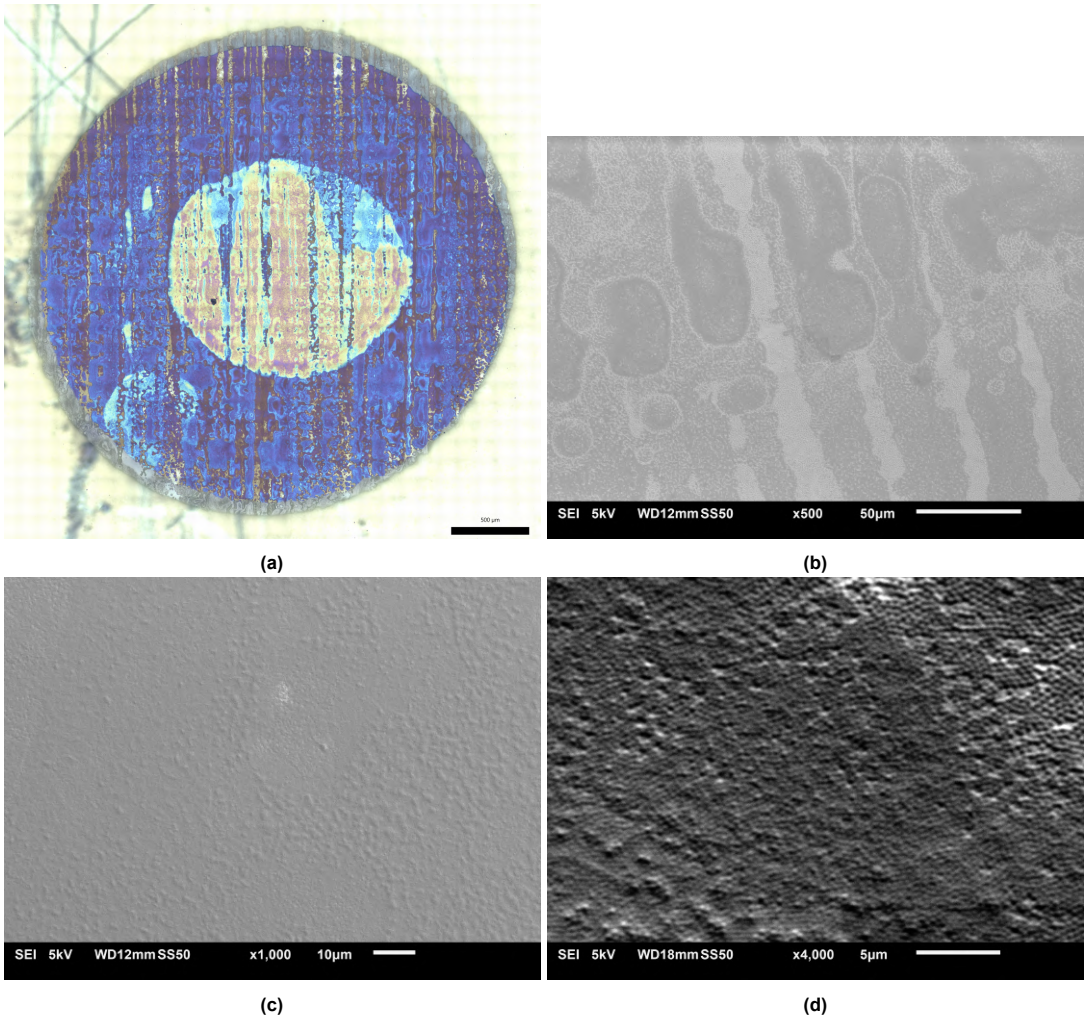

Figure 3.13: *a)* Optical microscope image showing a print of 1500 DPI 2 iterations, (*b*), (*c*) and (*d*) are SEM images at 500x, 1000x and 4000x magnification of a printed pNIPAm-TRT sample at a DPI of 1500 2 iterations. In *b* it shows that there appear to be two layers of pNIPAm particles, because of the two iterations of printing, but it still appears to be monolithic. However, *c* and *d* show a hill like structures. Thus implying a non monolithic layer.

3.2.3. Cleaning of the cartridge

The surface of the cartridge will get covered during printing, as seen in Figure 3.14. This is called wetting and this phenomena can occur when the printer settings are not set correctly. This can be the result of leakage or it can also be the result of air motion created by the jetting of the pNIPAm [49]. Figure 3.14a is the nozzle prior to pNIPAm-TRT deposition on the substrate. Figure 3.14b shows the nozzle after use. It shows that around the nozzle pNIPAm particles are agglomerating. The cleaning procedure consists of putting the cartridge in a tube filled with Milli-Q® water and put in a sonicator bath for 2 minutes, after which the water was disposed of. Most of the bead were removed after this treatment as can be seen in Figure 3.14c. The cartridge is stored in a tube filled with Milli-Q® water.

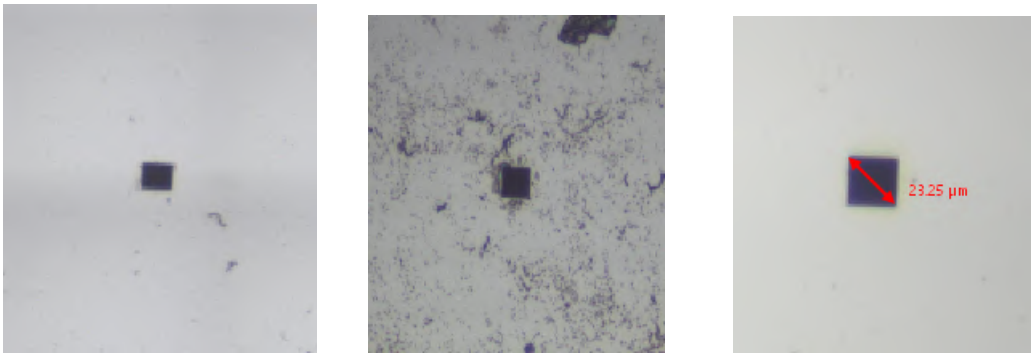

(a) (b) (c)

Figure 3.14: Clean nozzle (*a*) before use, (*b*) shows the nozzle after use. It can be seen that the area is covered with pNIPAm particles. It is therefore needed to clean the nozzle after each use. To clean the nozzle a sonicator for 2 minutes is used as seen in*c*.

3.3. Inkjet printed sample compared with spincoated sample

This section is dedicated to the comparison of spin coated samples with inkjet printed ones. Figure 3.15 shows both the sample that was spincoated with pNIPAm-TRT and the sample that deposited pNIPAm-TRT with the inkjet printer at a DPI of 4000. Both Figure 3.15a and Figure 3.15b show that a monolithic layer is formed. The monolithic layer formed by spincoating was expected for every sample that used this method see Appendix A FiguresA.3,A.6 and A.5. Based on these images it can be concluded that it is possible to form a monolithic layer by depositing pNIPAm with an inkjet printer.

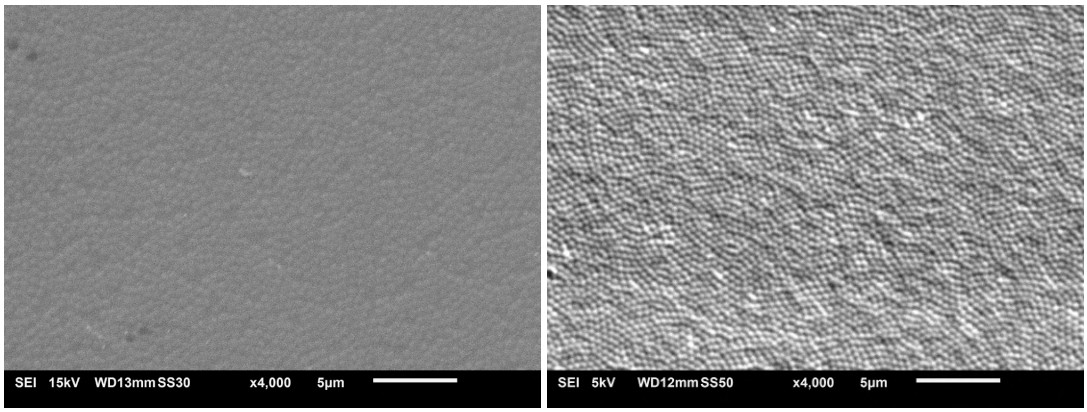

(a) (b)

Figure 3.15: SEM image of (*a*) Spincoated pNIPAm with Triton X-114 and (*b*) Inkjet printed pNIPAm with Triton X-114.

3.3.1. Print Consistency

During the printing part of this work it was noticed that the overall printing quality was not consistent. Figure 3.16 shows various printed samples. All these samples were printed with the same waveform seen in Figure 3.8b in paragraph 3.2.1. The only setting changed was the DPI. Figures 3.16a, 3.16b and 3.16c, show various printing results at a DPI of 1500. The golden substrate layer is clearly noticeable. The same can be said about Figures 3.16d, 3.16e and 3.16f. However, the gold is less noticeable. This is because of the increase in DPI from 1500 to 2000. It shows that the deposited pNIPAm cover more of the substrate. This inconsistency in coverage is probably a cause of non optimal print and waveform settings. To prevent this from happening further studies have to be conducted regarding the pNIPAm suspension and the printer settings. The best print results are done with a DPI of 4000, as can be seen in Figures 3.16g, 3.16h and 3.16i. All three show a cohesive ”single” drop. What is noticeable, the splashing around the edges of the print. Again, this is probably a cause of non optimal settings. This requires a study on what kind of print quality is needed.

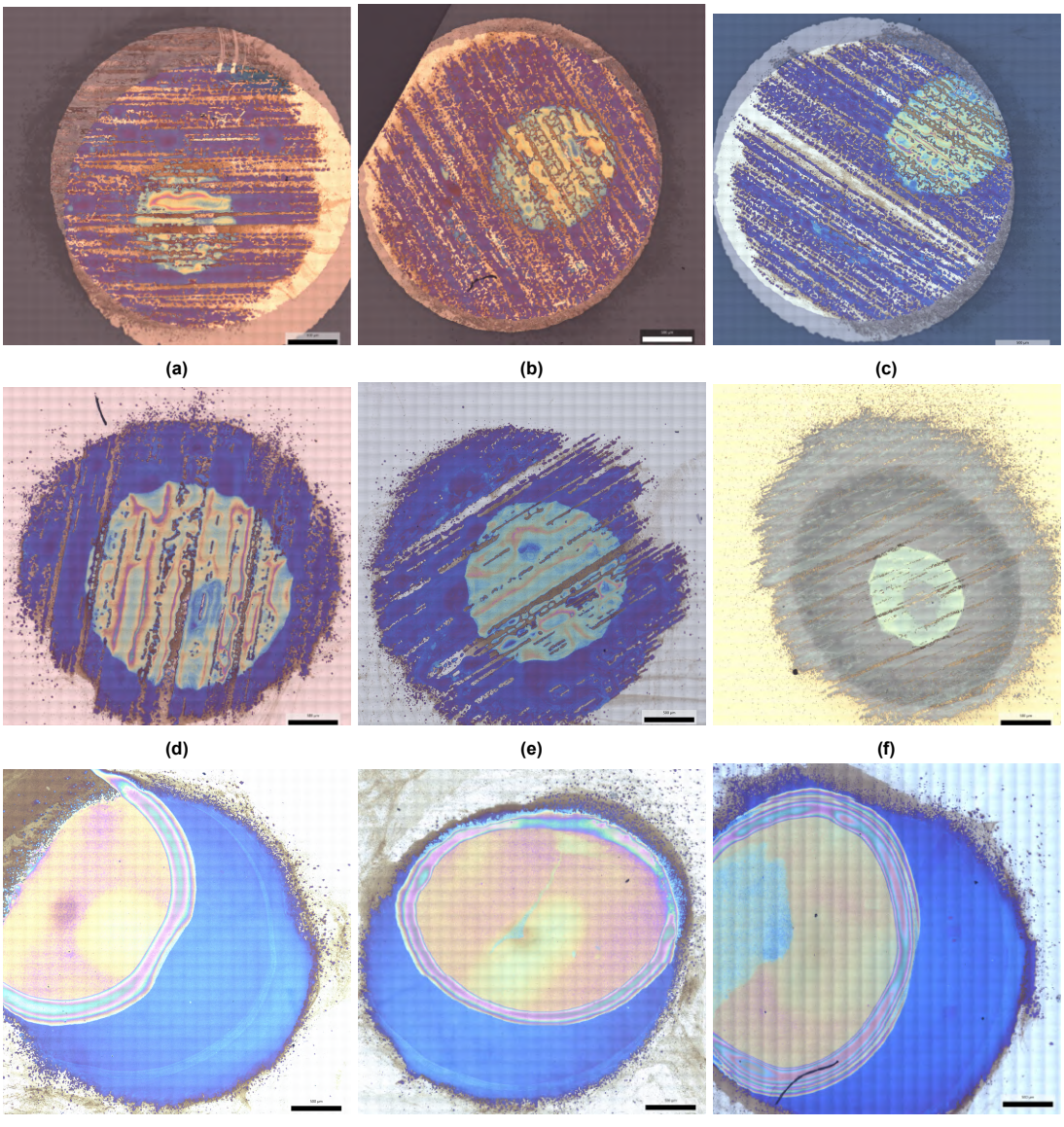

Figure 3.16: Print quality of $3\ mm$ samples with DPI of 1500(*a,b,c*), 2000(*d,e,f*) and 4000(*g,h,i*). At 1500 DPI the difference in quality is the most noticeable. There is no consistency where there is no pNIPAm deposit. Same can be said for the 2000 DPI. However, the consistency is more noticable. The gold substrate is more covered compared to the 1500 DPI. The 4000 DPI covers the substrate the best and shows the most consistency amongs the three different DPI's.

3.3.2. Gold/white spot removal

As shown in Figure3.16, each printed sample has a gold/white spot on it. This is a result of the rinsing step after depositing the pNIPAm-TRT on the substrate. As an affect of this step, residual water stayed on the deposited pNIPAm. When left to dry overnight, the next day this gold/white spot is formed at the location of the residual water. As shown in Figure A.7 in Appendix A, there is a difference in density. Besides the density, the gold/white spot shows that it is not a monolithic layer. To remove this spot various procedures have been tested, these are;

- Removing the residual water after rinsing with tissue paper
- Removing the residual water after rinsing with an Argon gun
- Removing the residual water after rinsing by putting the sample in a petri dish and fill it with Milli-Q® water and slowly tilt it and remove the drop by ”gravity”

All these procedures reduced the gold/white spot as seen in Figure3.17a, 3.17b and 3.17c. There is still some gold/white spots left. Further studies have to be conducted in implementing a procedure in making a microgel based etalon where the microgel is deposited with an inkjet printer.

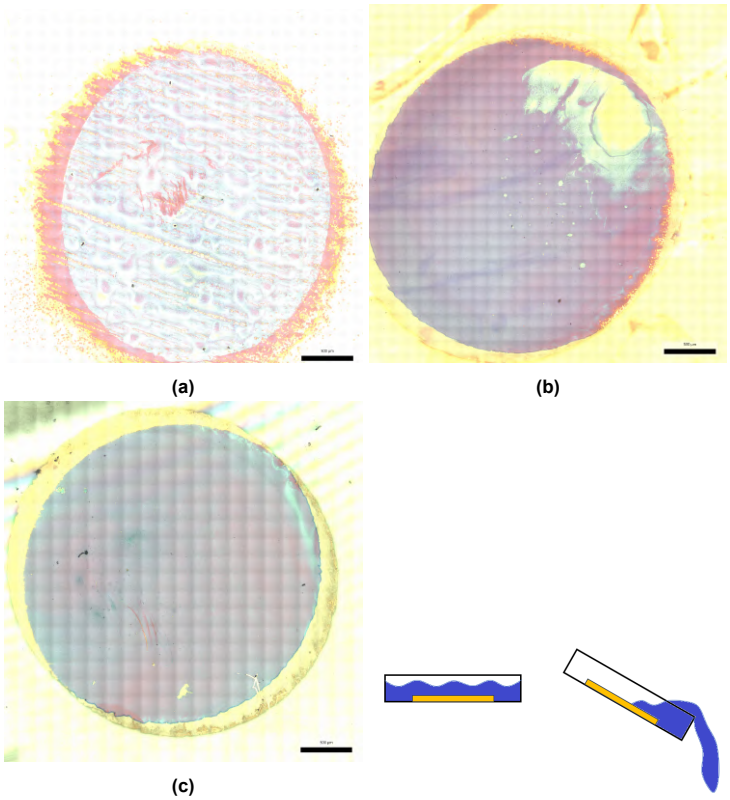

Figure 3.17: In (*a*) the sample, the residual water is removed by a tip of tissue paper. (*b*) the residual water is removed by blowing argon of the deposited pNIPAm-TRT. It shows that the majority of the gold/white is removed using this method. The last method (*d*) was putting the sample in a small petri dish and fill it with Milli-Q® and slowly remove the water by tilting the petri dish until all the water is removed. This methods shows that the drop in (*c*) is almost completely removed.

Results & Discussion: Reflectance Spectroscopy

3.4. Reflectance spectroscopy results

As mentioned in chapter 1 the pNIPAm microgel are thermo-responsive. To test its responsiveness reflectance spectroscopy experiments are conducted. The expected results should behave similar as in the paper by *Andrews Ahiabu and Michael J. Serpe*, 2017 [50]. The peak wavelength should decrease when the temperature increases and that it will eventually reach a plateau. This plateau means that increasing the temperature will not result in a further peak shift because the particles are in the complete deswollen state. Figure 3.18 shows the results of various DPI's that have been printed. The graph shows the $\Delta\lambda$ of the peak shifts. Which is the difference in peak shift where the peak at 20°C is considered the base line. In appendix A FigureA.11 till A.18 shows the reflectance and intensity vs the wavelength. Which are used to determine the $\Delta\lambda$. Figure 3.18a, 3.18c, 3.18b and 3.18d shows $\Delta\lambda$ peak shift of the samples that were made at a DPI of 1500, 2000, two iterations of 1500 and 4000 respectively. These figures show that there is a shift towards the blue spectra when the temperature increases. Which means the $\Delta\lambda$ decreases due to the deswelling of the pNIPAm particles. When the temperature reaches 40°C and higher, a plateau is reached. This is in correspondence with the literature found [50, 11]. It can therefore be said that using an inkjet printer to deposit pNIPAm on a substrate is a viable alternative to spincoating or "painting-on" method [11].

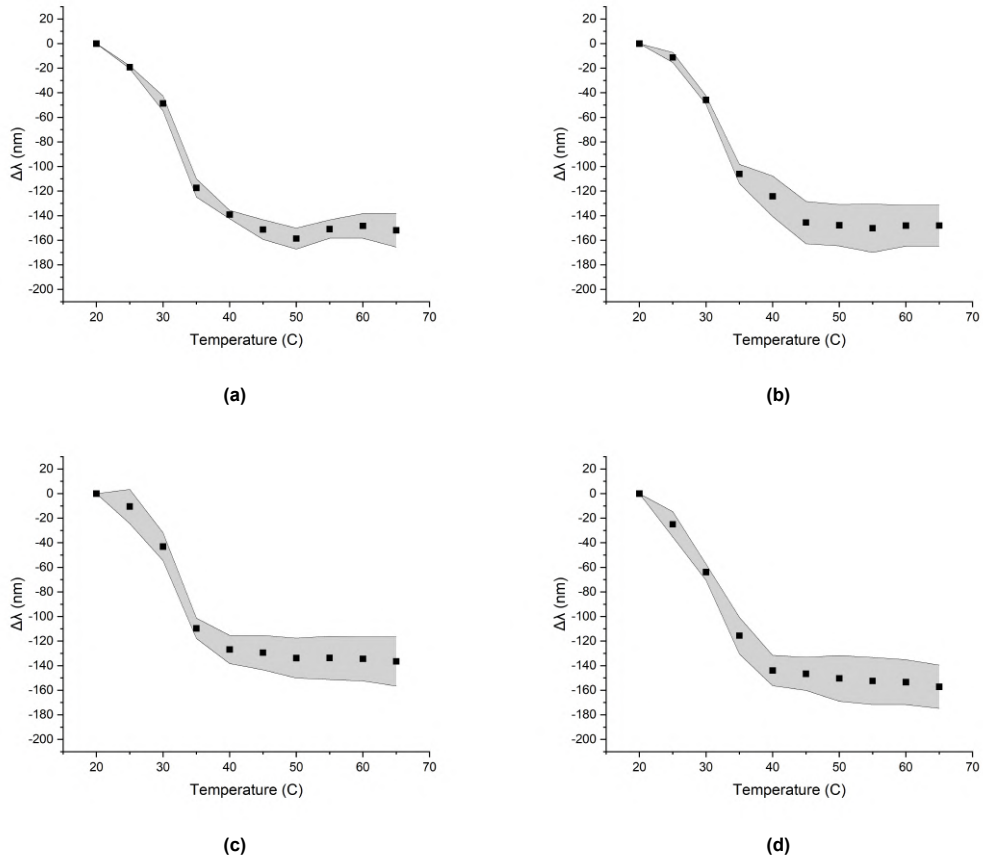

Figure 3.18: Reflectance spectroscopy results of the peak shift. (*a*) 1500 DPI, (*b*) 1500 DPI 2 iterations, (*c*) 2000 DPI and (*d*) 4000 DPI. They all show a decrease in $\Delta\lambda$. This due to the fact that the pNIPAm particles deswell when the temperature increases. When the temperature reaches 45°C and up, a plateau is reached. Because the pNIPAm particles do not deswell further beyond this point.

4

Conclusion

There were two points that needed to be investigated at the start of this thesis. The first one was the possibility to deposit pNIPAm on a substrate by using an inkjet printed as depositing mechanism. The second point was, if there will be a peak shift in the wavelength number when the temperature increases, just like spincoating or ”painting-on” methods of applying pNIPAm.

To answer the first question it was needed to characterise the physical properties of the pNIPAm suspension that is used. This suspension had to be within range of the requirements of the *Dimatix* cartridge Table 2.1. To lower the surface tension, three surfactants have been chosen; Triton X-114 (TRT), Sodium Dodecyl Sulphate (SDS) and Hexadecyltrimethylammonium bromide (CTAB). It is known that surfactants lower the surface tension but it was also necessary to investigate if they had any influence on the density, the pNIPAm particle size and the viscosity. The surfactants had little to no influence on the measured density, the particle size and the viscosity. Of the three surfactants; TRT, SDS and CTAB, TRiton X-114 was the surfactant that lowered the surface tension the most From $67,44\ mN/m$ to $38,39\ mN/m$ at 20 °C and $66,37\ mN/m$ to $37,04\ mN/m$ at 45 °C from . Based on these results it was decided that TRT is the surfactant that will be used to see if pNIPAm is jettable with an inkjet printer. With these characterisations it is also possible to determine the minimum velocity needed to produce a drop, to overcome the surface tension at the nozzle. The minimum velocity needed is $2,57$ m/s. The Ohnesorge and Reynolds number derived from these characteristics were to low to produce a drop. Not enough energy is produced to form a drop. Hence it was necessary to change the waveform setting of the inkjet printer. This resulted in a measured velocity of $5,70\ m/s$, which is enough to overcome the surface tension but also enough to come into the region of drop formation.

To simplify the answer to the question; *Is it possible to deposit pNIPAm by using an inkjet printer*, the answer is **yes**. It is possible to deposit pNIPAm on a substrate. However, consistency is a problem. The inkjet printer did not deliver the same quality for each print, the end result varied from sample to sample. This is especially the case for prints with a DPI of 1500 or 2000. But this difference in quality could be a cause of the fact that the pNIPAm is on the border of producing satellite drops. The theory suggest that satellite drops will be formed if the Ohnesorge(Oh) Number is lower than $0,1$. The measured Oh number at temperatures of 30 and 35°C of the pNIPAm-TRT is between $0,091$ and $0,069$. When the DPI is 4000, there is consistency. Each of the 4000 DPI samples look the same under the SEM. One consistency that each sample has is a gold/white spot on the deposited pNIPAm. This spot is likely caused by residual water after rinsing it with Milli-Q® water. Several attempts have been made to remove this residual water thus reducing this drop. This is possible however a proper procedure has to be constructed to be consistent.

The last part of the project was to see if there is a peak shift in the wavelength when the temperature is increased. Literature shows that there will be a peak shift when pNIPAm is applied with methods like spincoating or paint-on method. This shift is caused by the swelling and de-swelling of the pNIPAm particles. The peak shift was observerd in the inkjet printed samples with increase of the temperature. It even shows that a plateau is reached when the temperature is increased further than 40, 45 °C. This

plateau is reached because the pNIPAm does not de-swell any further after these temperatures. It was also observed that there is no difference when it comes to printing in 1500, 2000 or 4000 DPI. Even printing twice over the same location shows the same kind of trend. The only sample that was unable to show this trend was the one with a DPI of 500. This was mainly due to the fact that the used reflectance spectrometer was not sensitive enough and that there was too much space between each deposited drop and the substrate layer. Overall this project can be seen as a success. It is possible to use an inkjet printer to deposit pNIPAm and it behaves as expected. This method of applying pNIPAm will bring various new opportunities to the usage of pNIPAm. For example for Organ-On-Chip application. For instance, it is not necessary anymore to use masks to prevent pNIPAm from going to places where it is not needed and/or welcome. Inkjet printing gives the opportunity to deposit precisely and in small quantities pNIPAm on substrates, which means that Organ-on-Chip designs can also be reconsidered by not taking spincoating or ”pain-on” method into designing criteria.

5

Recommendations

5.1. pNIPAm INK and Inkjet printing

Printing and creating a monolithic layer of pNIPAm is achieved but the pNIPAm "*ink*" can be optimized. This thesis focused on just three surfactants, there could be surfactants that lower the surface tension more than what was achieved in Chapter 3. For example for;

- Anoionic surfactant: Docusate, this is a surfactant that is already used in medicine.
- Cationic surfactant: Cetylpyridinium chloride, this surfactant is an antiseptic that is used in mouth-wash.
- Non-ionic surfactant: Tweens or Polysorbate, these surfactants are used in the pharmaceutical and food industry.
- Amphoteric surfactant: Myristamine oxide, which is a surfactant used in shampoos and or conditioners.

Also what can be researched is the effect of increasing or decreasing the concentration of pNIPAm beads. As mentioned this was kept consistent throughout the whole thesis to reduce the number of variables. Besides the ink optimization the printing itself can also be optimized. As seen in Chapter 3.1.7, the overall quality of the print is not consistent. To create consistency, a further investigation has to be done on the settings of the inkjet printer. It is also important to define what the overall quality should be with the prints. Does it matter that there is some splashing or is it needed that the edges of the print are tidy and neat. Another aspect that needs to be investigated, is how to remove the gold/white spots on the printed samples. Some trials have been conducted and there is limited success in the removing of the gold/white spot. Therefore, a procedure has to be developed how to produce printed microgel based etalons.

5.2. Application of the inkjet printed pNIPAm

Now that it is possible to deposit pNIPAm with an inkjet printer. It is needed to investigate where this can be applied. Is it possible to use this method when it comes to applying pNIPAm on an Organ-On-Chip. If this will be used for OoC then it is important to keep the surrounding atmosphere controlled, hence it should be moved to a cleanroom.

References

[1] Robert Pelton. “Temperature-sensitive aqueous microgels”. In: *Advances in Colloid and Interface Science* 85.1 (2000), pp. 1–33. ISSN: 0001-8686. DOI: https://doi.org/10.1016/S0001-8686(99)00023-8. URL: https://www.sciencedirect.com/science/article/pii/S0001868699000238.

[2] H.G. Schild. “Poly(N-isopropylacrylamide): experiment, theory and application”. In: *Progress in Polymer Science* 17.2 (1992), pp. 163–249. ISSN: 0079-6700. DOI: https://doi.org/10.1016/0079-6700(92)90023-R. URL: https://www.sciencedirect.com/science/article/pii/007967009290023R.

[3] Martien A Cohen Stuart et al. “Emerging applications of stimuli-responsive polymer materials”. en. In: *Nat Mater* 9.2 (Jan. 2010), pp. 101–113.

[4] Garima Agrawal and Rahul Agrawal. “Stimuli-Responsive Microgels and Microgel-Based Systems: Advances in the Exploitation of Microgel Colloidal Properties and Their Interfacial Activity”. In: *Polymers* 10.4 (Apr. 2018), p. 418. DOI: 10.3390/polym10040418. URL: https://doi.org/10.3390/polym10040418.

[5] Jayanta Kumar Patra et al. “Nano based drug delivery systems: recent developments and future prospects”. In: *Journal of Nanobiotechnology* 16.1 (Sept. 2018), p. 71.

[6] Changhai Ru et al. “A review of non-contact micro- and nano-printing technologies”. In: *Journal of Micromechanics and Microengineering* 24.5 (Apr. 2014), p. 053001. DOI: 10.1088/0960-1317/24/5/053001. URL: https://dx.doi.org/10.1088/0960-1317/24/5/053001.

[7] *HP Deskjet Printer, 1988*. URL: https://www.hp.com/hpinfo/abouthp/histnfacts/museum/imagingprinting/0019/index.html.

[8] William Elward. *Inkjet printer history*. Oct. 2019. URL: https://castleink.com/blogs/printer-help/inkjet-printer-history.

[9] Fulvia Villani et al. “Inkjet Printed Polymer Layer on Flexible Substrate for OLED Applications”. In: *The Journal of Physical Chemistry C* 113.30 (2009), pp. 13398–13402. DOI: 10.1021/jp8095538. eprint: https://doi.org/10.1021/jp8095538. URL: https://doi.org/10.1021/jp8095538.

[10] Ian. Hutchings. *Inkjet technology for digital fabrication*. English. Chichester: Wiley, 2013.

[11] Courtney D. Sorrell, Matthew C. D. Carter, and Michael J. Serpe. “A “Paint-On” Protocol for the Facile Assembly of Uniform Microgel Coatings for Color Tunable Etalon Fabrication”. In: *ACS Applied Materials & Interfaces* 3.4 (2011). PMID: 21381654, pp. 1140–1147. DOI: 10.1021/am1012722. URL: https://doi.org/10.1021/am1012722.

[12] Molla R. Islam et al. “Poly (N-isopropylacrylamide) Microgel-Based Optical Devices for Sensing and Biosensing”. In: *Sensors* 14.5 (2014), pp. 8984–8995. ISSN: 1424-8220. DOI: 10.3390/s140508984. URL: https://www.mdpi.com/1424-8220/14/5/8984.

[13] *LP50 Inkjet Printer | SUSS MicroTec — suss.com*. https://www.suss.com/en/products-solutions/inkjet-printing/lp50. [Accessed 18-03-2023].

[14] David Quéré. “Wetting and Roughness”. In: *Annual Review of Materials Research* 38.1 (2008), pp. 71–99. DOI: 10.1146/annurev.matsci.38.060407.132434. eprint: https://doi.org/10.1146/annurev.matsci.38.060407.132434. URL: https://doi.org/10.1146/annurev.matsci.38.060407.132434.

[15] Lei Xu, Wendy W. Zhang, and Sidney R. Nagel. “Drop Splashing on a Dry Smooth Surface”. In: *Phys. Rev. Lett.* 94 (18 May 2005), p. 184505. DOI: 10.1103/PhysRevLett.94.184505. URL: https://link.aps.org/doi/10.1103/PhysRevLett.94.184505.

[16] Dirkjan Dam and Christophe Le Clerc. “Experimental study of the impact of an ink-jet printed droplet on a solid substrate”. In: *Physics of Fluids* 16 (Aug. 2004). DOI: 10.1063/1.1773551.

[17] Hansol Yoo and Chongyoup Kim. “Experimental studies on formation, spreading and drying of inkjet drop of colloidal suspensions”. In: *Colloids and Surfaces A: Physicochemical and Engineering Aspects* 468 (2015), pp. 234–245. ISSN: 0927-7757. DOI: https://doi.org/10.1016/j.colsurfa.2014.12.032. URL: https://www.sciencedirect.com/science/article/pii/S0927775714009522.

[18] Chr. Mundo, M. Sommerfeld, and C. Tropea. “Droplet-wall collisions: Experimental studies of the deformation and breakup process”. In: *International Journal of Multiphase Flow* 21.2 (1995), pp. 151–173. ISSN: 0301-9322. DOI: https://doi.org/10.1016/0301-9322(94)00069-V. URL: https://www.sciencedirect.com/science/article/pii/030193229400069V.

[19] Boonkhong Kittipat, Montri Karnjanadecha, and Pattara Aiyarak. “Impact angle analysis of bloodstains using a simple image processing technique”. In: *Songklanakarin Journal of Science and Technology* 32 (May 2010).

[20] Pei He and Brian Derby. “Controlling Coffee Ring Formation during Drying of Inkjet Printed 2D Inks”. In: *Advanced Materials Interfaces* 4.22 (2017), p. 1700944. DOI: https://doi.org/10.1002/admi.201700944. eprint: https://onlinelibrary.wiley.com/doi/pdf/10.1002/admi.201700944. URL: https://onlinelibrary.wiley.com/doi/abs/10.1002/admi.201700944.

[21] Rafal Sliz, Jakub Czajkowski, and Tapio Fabritius. “Taming the Coffee Ring Effect: Enhanced Thermal Control as a Method for Thin-Film Nanopatterning”. In: *Langmuir* 36.32 (Aug. 2020), pp. 9562–9570. ISSN: 0743-7463. DOI: 10.1021/acs.langmuir.0c01560. URL: https://doi.org/10.1021/acs.langmuir.0c01560.

[22] Thu Thi Yen Le, Siam Hussain, and Shi-Yow Lin. “A study on the determination of the critical micelle concentration of surfactant solutions using contact angle data”. In: *Journal of Molecular Liquids* 294 (2019). Cited by: 14. DOI: 10.1016/j.molliq.2019.111582. URL: https://www.scopus.com/inward/record.uri?eid=2-s2.0-85070983417%5C&doi=10.1016%5C%2fj.molliq.2019.111582%5C&partnerID=40%5C&md5=0feaa4b11c21235801f429e8230a73df.

[23] Detlef Lohse. “Fundamental Fluid Dynamics Challenges in Inkjet Printing”. English. In: *Annual review of fluid mechanics* 54 (Jan. 2022). Publisher Copyright: © 2021 Annual Reviews Inc.. All rights reserved., pp. 349–382. ISSN: 0066-4189. DOI: 10.1146/annurev-fluid-022321-114001.

[24] Harishankar Manikantan and Todd M. Squires. “Surfactant dynamics: hidden variables controlling fluid flows”. In: *Journal of Fluid Mechanics* 892 (2020), P1. DOI: 10.1017/jfm.2020.170.

[25] Boris Zhmud and Fredrik Tiberg. “Surfactants in Ink-Jet Inks”. In: Jan. 2003. ISBN: 9781841273365. DOI: 10.1201/9780367812416-8.

[26] Gianmarco Venditti, Vignesh Murali, and Anton A. Darhuber. “Inkjet printing of surfactant solutions onto thin moving porous media”. In: *Colloids and Surfaces A: Physicochemical and Engineering Aspects* 634 (2022), p. 127832. ISSN: 0927-7757. DOI: https://doi.org/10.1016/j.colsurfa.2021.127832. URL: https://www.sciencedirect.com/science/article/pii/S0927775721017015.

[27] Brian Derby. “Inkjet Printing of Functional and Structural Materials: Fluid Property Requirements, Feature Stability, and Resolution”. In: vol. 40. June 2010, pp. 395–414. DOI: 10.1146/annurev-matsci-070909-104502.

[28] Gareth McKinley and Michael Renardy. “Wolfgang von Ohnesorge”. In: *Physics of Fluids* 23 (Dec. 2011). DOI: 10.1063/1.3663616.

[29] Paul Duineveld et al. “Ink-jet printing of polymer light-emitting devices”. In: *Proc. SPIE* 4464 (Feb. 2002). DOI: 10.1117/12.457460.

[30] Deepak Gupta et al. “Temperature-driven volume phase transition of a single stimuli-responsive microgel particle using optical tweezers”. In: *Colloid and Polymer Science* 294 (Dec. 2016). DOI: 10.1007/s00396-016-3952-1.

[31] Zahoor H. Farooqi et al. “Stability of poly(N-isopropylacrylamide-co-acrylic acid) polymer microgels under various conditions of temperature, pH and salt concentration”. In: *Arabian Journal of Chemistry* 10.3 (2017), pp. 329–335. ISSN: 1878-5352. DOI: https://doi.org/10.1016/j.arabjc.2013.07.031. URL: https://www.sciencedirect.com/science/article/pii/S1878535213002311.

[32] Courtney Sorrell and Michael Serpe. “Reflection Order Selectivity of Color-Tunable Poly(N-isopropylacrylamide) Microgel Based Etalons”. In: *Advanced materials (Deerfield Beach, Fla.)* 23 (Sept. 2011), pp. 4088–92. DOI: 10.1002/adma.201101717.

[33] Brian Derby. “Inkjet Printing of Functional and Structural Materials: Fluid Property Requirements, Feature Stability, and Resolution”. In: *Annual Review of Materials Research* 40.1 (2010), pp. 395–414. DOI: 10.1146/annurev-matsci-070909-104502. eprint: https://doi.org/10.1146/annurev-matsci-070909-104502. URL: https://doi.org/10.1146/annurev-matsci-070909-104502.

[34] W. Zapka. *Inkjet Printing in Industry: Materials, Technologies, Systems, and Applications*. Wiley, 2022. ISBN: 9783527347803. URL: https://books.google.nl/books?id=w-faywEACAAJ.

[35] Mohmed Mulla et al. “Colloid Particles in Ink Formulations”. In: Dec. 2015, pp. 141–168. ISBN: 9783527337859. DOI: 10.1002/9783527684724.ch6.

[36] URL: https://www.sigmaaldrich.com/NL/en/product/sial/x114.

[37] URL: https://www.sigmaaldrich.com/NL/en/product/sigma/h5882.

[38] URL: https://www.sigmaaldrich.com/NL/en/product/sial/436143.

[39] Stephen D. Hoath. *Fundamentals of Inkjet Printing - the science of inkjet and droplets*. Wiley-vch Verlag Gmbh, 2016.

[40] Pijush K. Kundu et al. *Fluid mechanics*. Academic Press, 2016.

[41] John A. Roberson, D. F. Elger, and Clayton T. Crowe. *Engineering Fluid Mechanics*. Jan. 2019.

[42] G. Ovarlez. “2 - Introduction to the rheometry of complex suspensions”. In: *Understanding the Rheology of Concrete*. Ed. by Nicolas Roussel. Woodhead Publishing Series in Civil and Structural Engineering. Woodhead Publishing, 2012, pp. 23–62. ISBN: 978-0-85709-028-7. DOI: https://doi.org/10.1533/9780857095282.1.23. URL: https://www.sciencedirect.com/science/article/pii/B9780857090287500029.

[43] Alvaro Marin et al. “Clogging in constricted suspension flows”. In: *Phys. Rev. E* 97 (2 Feb. 2018), p. 021102. DOI: 10.1103/PhysRevE.97.021102. URL: https://link.aps.org/doi/10.1103/PhysRevE.97.021102.

[44] Ajeet Kumar and Chandra Kumar Dixit. “3 - Methods for characterization of nanoparticles”. In: (2017). Ed. by Surendra Nimesh, Ramesh Chandra, and Nidhi Gupta, pp. 43–58. DOI: https://doi.org/10.1016/B978-0-08-100557-6.00003-1. URL: https://www.sciencedirect.com/science/article/pii/B9780081005576000031.

[45] Tharwat Tadros. “General Principles of Colloid Stability and the Role of Surface Forces”. In: *Colloid Stability*. John Wiley & Sons, Ltd, 2006. Chap. 1, pp. 1–22. ISBN: 9783527631070. DOI: https://doi.org/10.1002/9783527631070.ch1. eprint: https://onlinelibrary.wiley.com/doi/pdf/10.1002/9783527631070.ch1. URL: https://onlinelibrary.wiley.com/doi/abs/10.1002/9783527631070.ch1.

[46] Katarzyna Szymczyk and Anna Taraba. “Aggregation behavior of Triton X-114 and Tween 80 at various temperatures and concentrations studied by density and viscosity measurements”. In: *Journal of Thermal Analysis and Calorimetry* 126 (July 2016). DOI: 10.1007/s10973-016-5631-3.

[47] Michael Johnston and Randy Ewoldt. “Precision rheometry: Surface tension effects on low-torque measurements in rotational rheometers”. In: *Journal of Rheology* 57 (Nov. 2013), p. 1515. DOI: 10.1122/1.4819914.

[48] Anna Burmistrova et al. “The Effect of Co-Monomer Content on the Swelling/Shrinking and Mechanical Behaviour of Individually Adsorbed PNIPAM Microgel Particles”. In: *Polymers* 3.4 (2011), pp. 1575–1590. ISSN: 2073-4360. DOI: 10.3390/polym3041575. URL: https://www.mdpi.com/2073-4360/3/4/1575.

[49] Saeed Fathi and Philip Dickens. “Nozzle Wetting and Instabilities During Droplet Formation of Molten Nylon Materials in an Inkjet Printhead”. In: *Journal of Manufacturing Science and Engineering* 134 (July 2012), pp. 041008–041008. DOI: 10.1115/1.4006971.

[50] Andrews Ahiabu and Michael Serpe. “Rapidly Responding pH- and Temperature-Responsive Poly (N -Isopropylacrylamide)-Based Microgels and Assemblies”. In: *ACS Omega* 2 (May 2017), pp. 1769–1777. DOI: 10.1021/acsomega.7b00103.

A

Appendix A

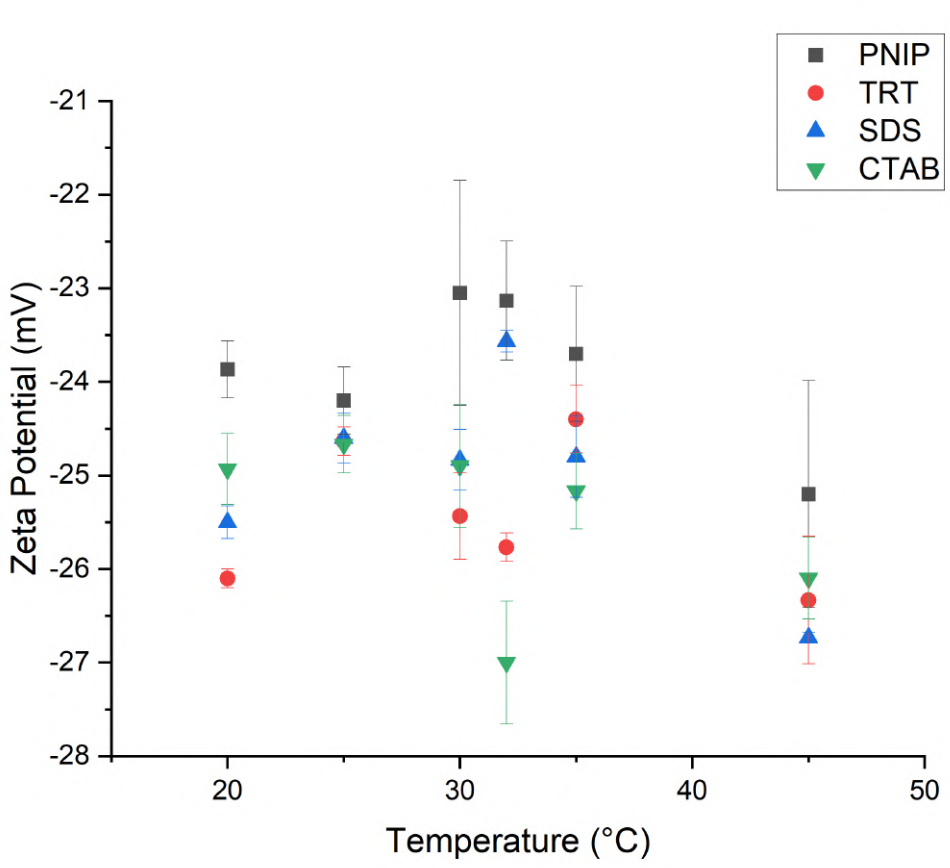

Figure A.1: Zetapotential of pNIPAm, pNIPAm-TRT pNIPAm-SDS and pNIPAm-CTAB.

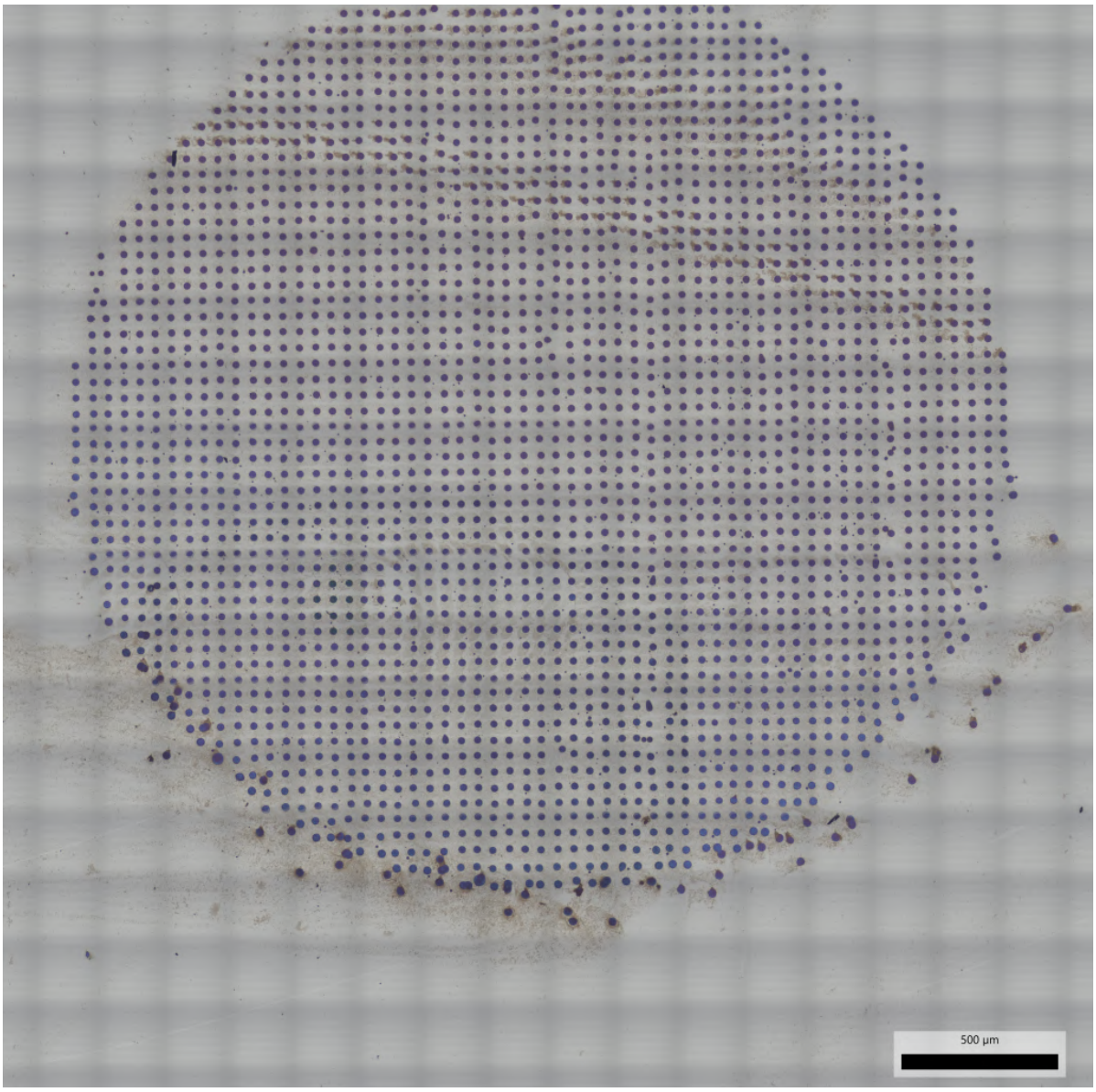

Figure A.2: $3\ mm$ diameter print at 500 DPI.

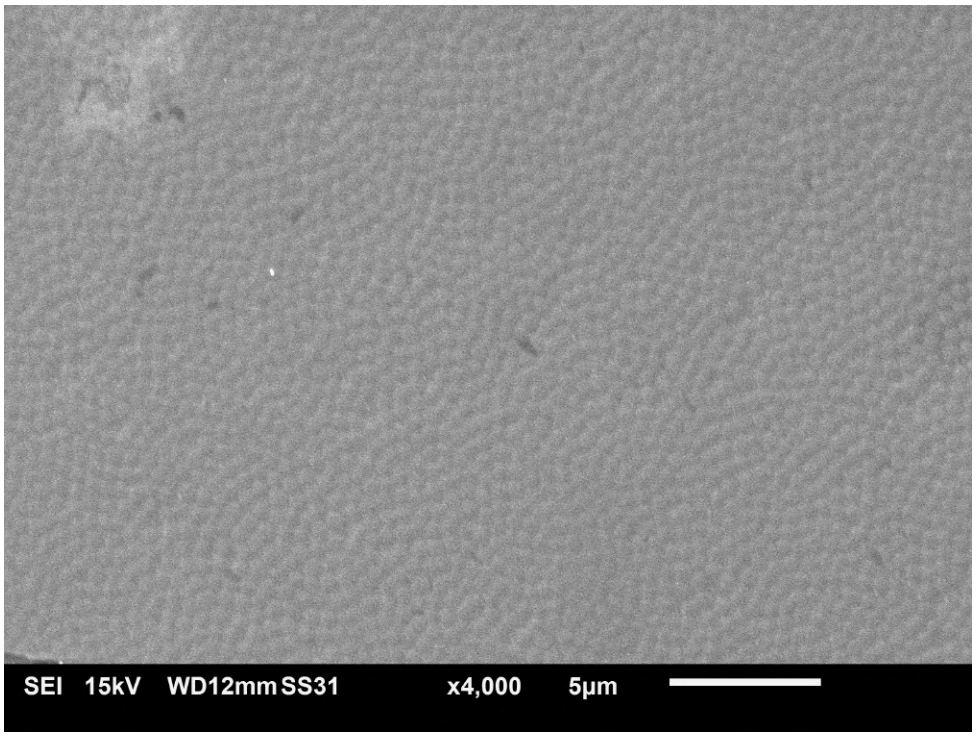

Figure A.3: PNIPAM applied by spincoating.

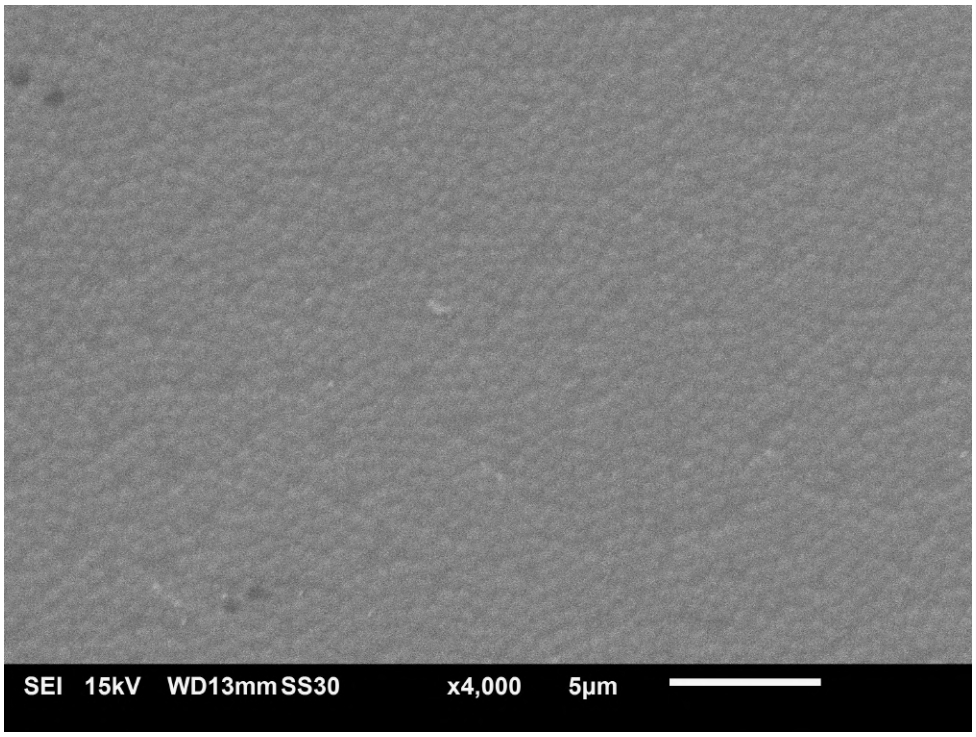

Figure A.4: PNIPAM + Triton X114 applied by spincoating.

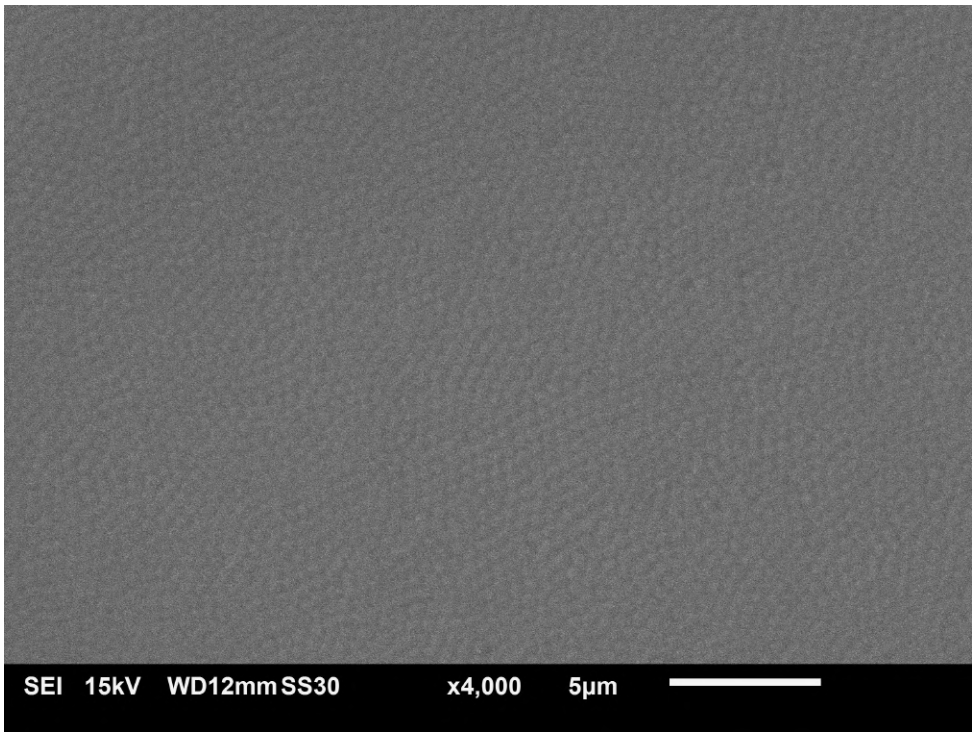

Figure A.5: PNIPAM + SDS applied by spincoating.

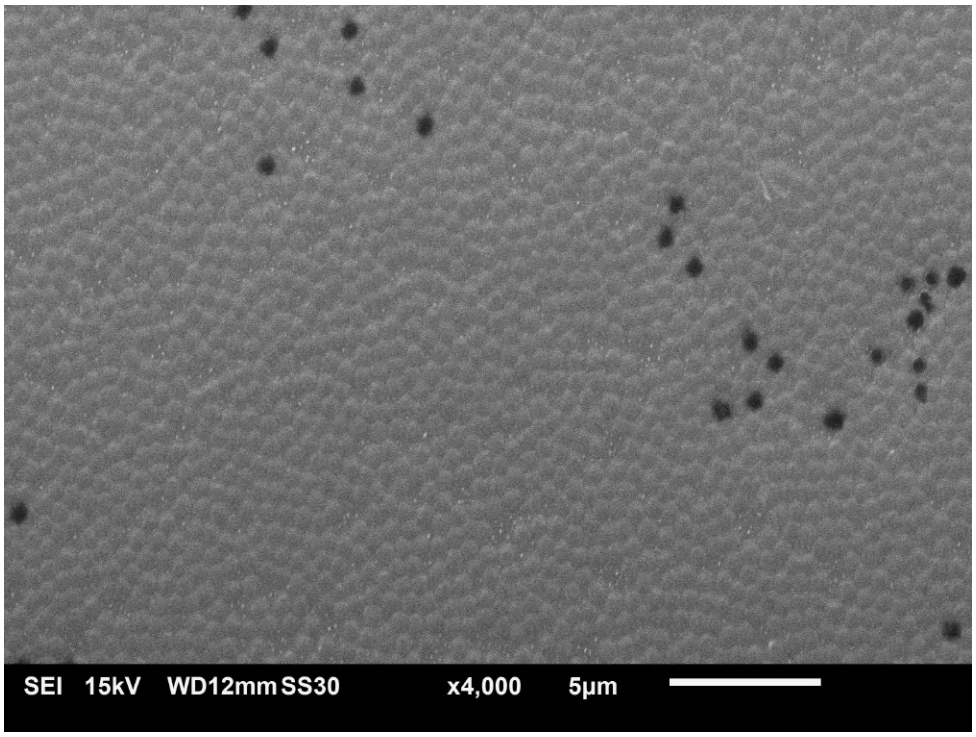

Figure A.6: PNIPAM + CTAB applied by spincoating.

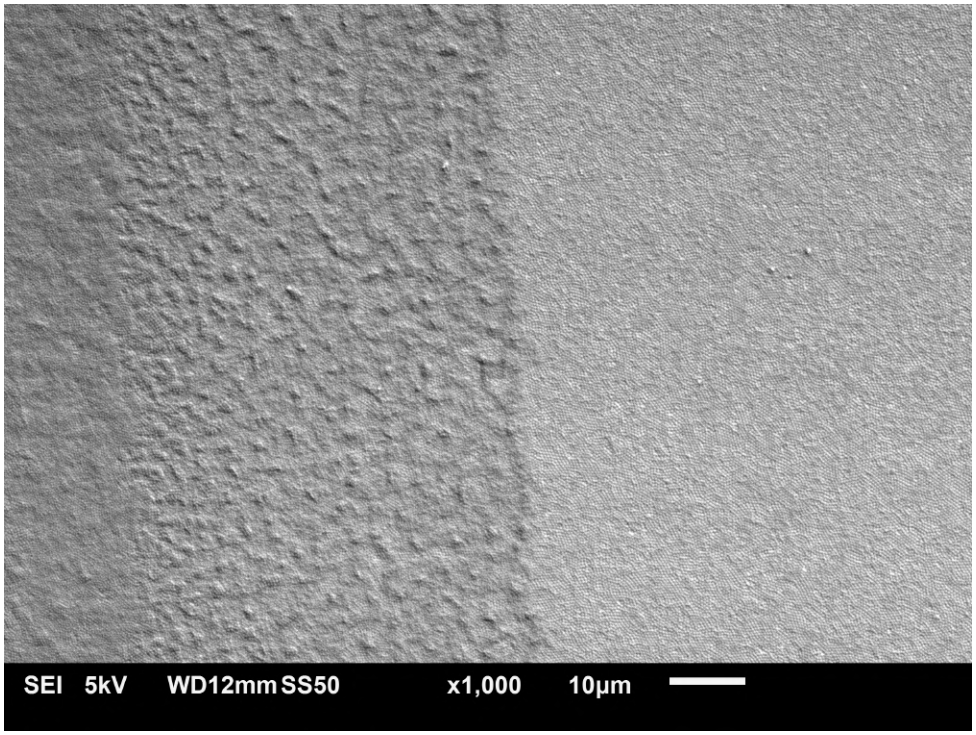

Figure A.7: pNIPAm density difference on the border of a gold/white spot.

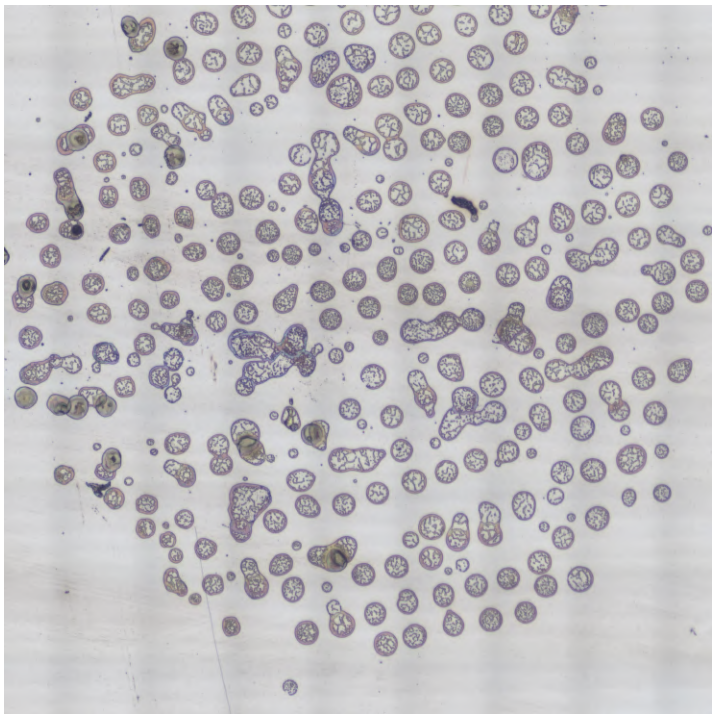

Figure A.8: Result of trial and error in finding the right waveform.

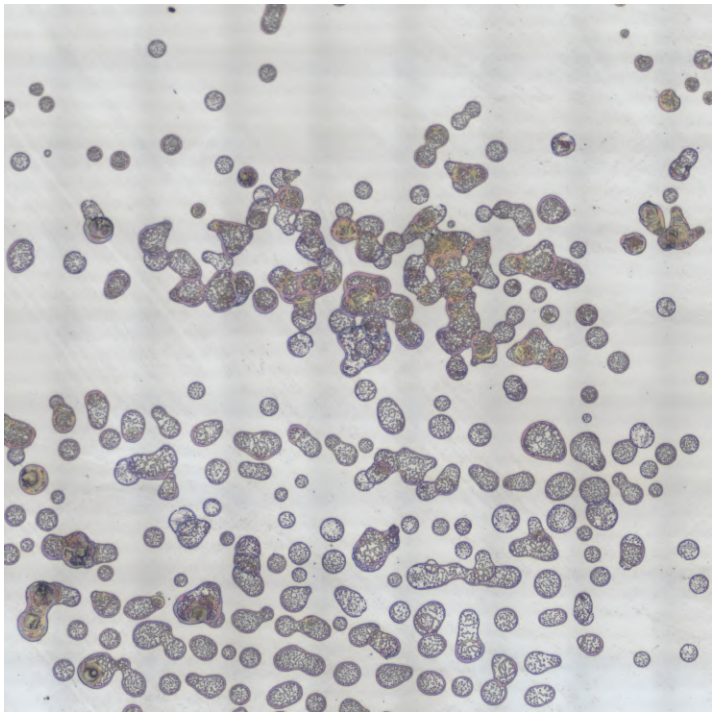

Figure A.9: Result of trial and error in finding the right waveform.

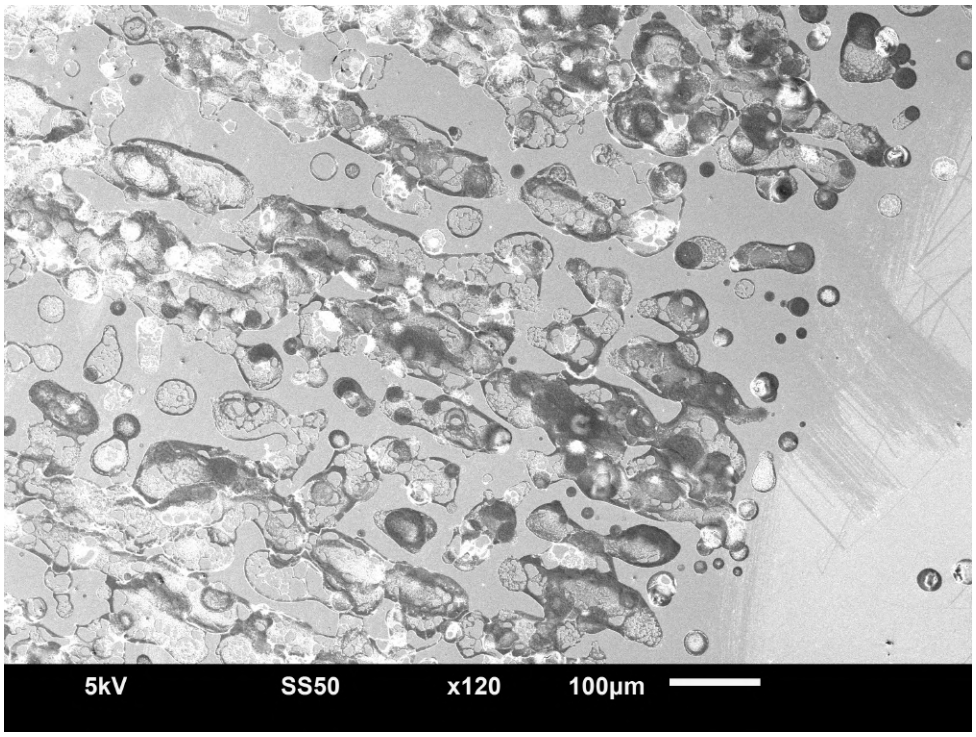

Figure A.10: Result of trial and error in finding the right waveform.

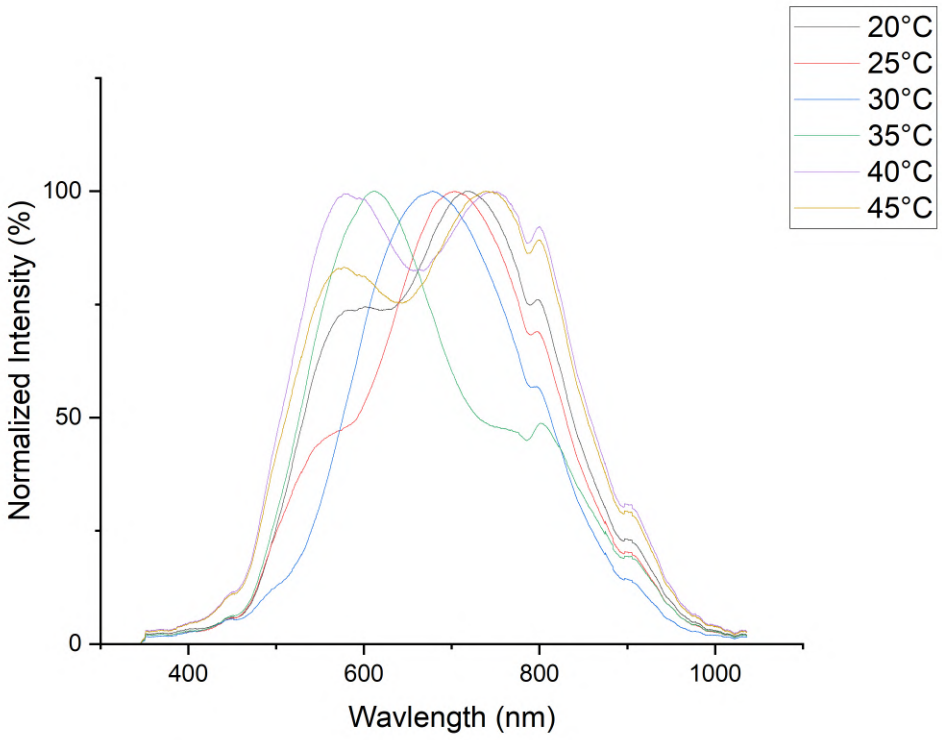

Figure A.11: 1500 DPI Normalized intensity vs Wavelength.

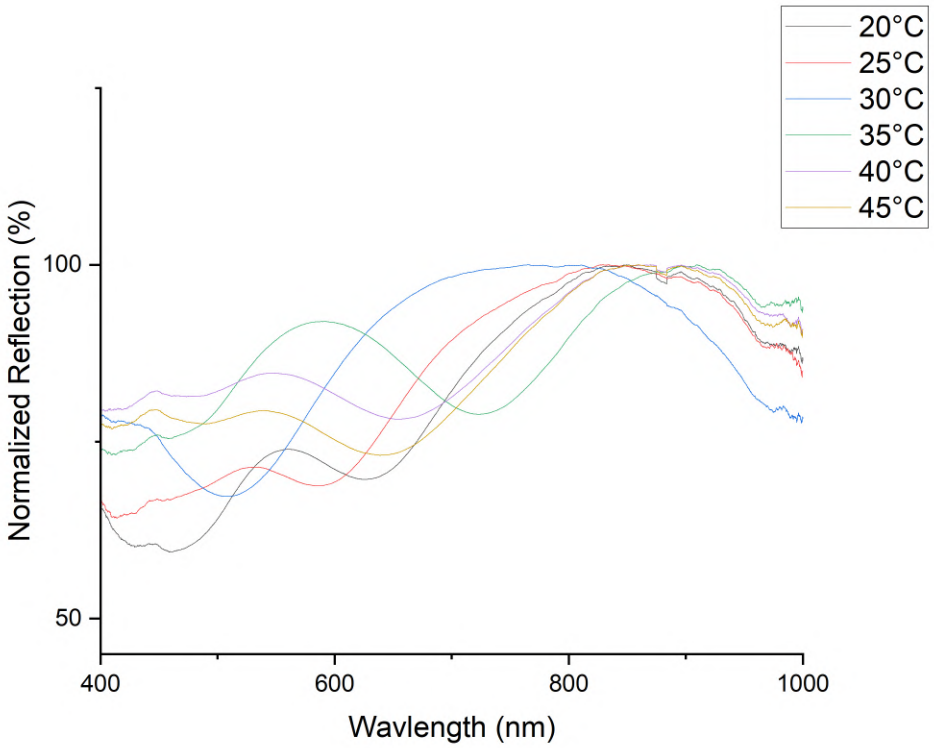

Figure A.12: 1500 DPI Normalized reflection vs Wavelength.

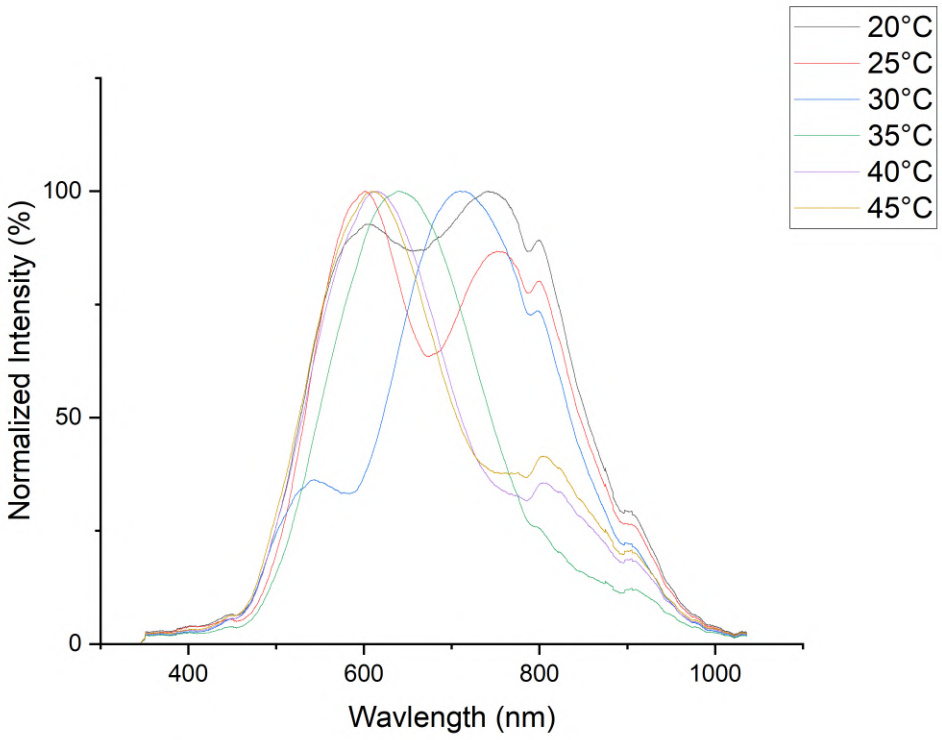

Figure A.13: 2000 DPI Normalized intensity vs Wavelength.

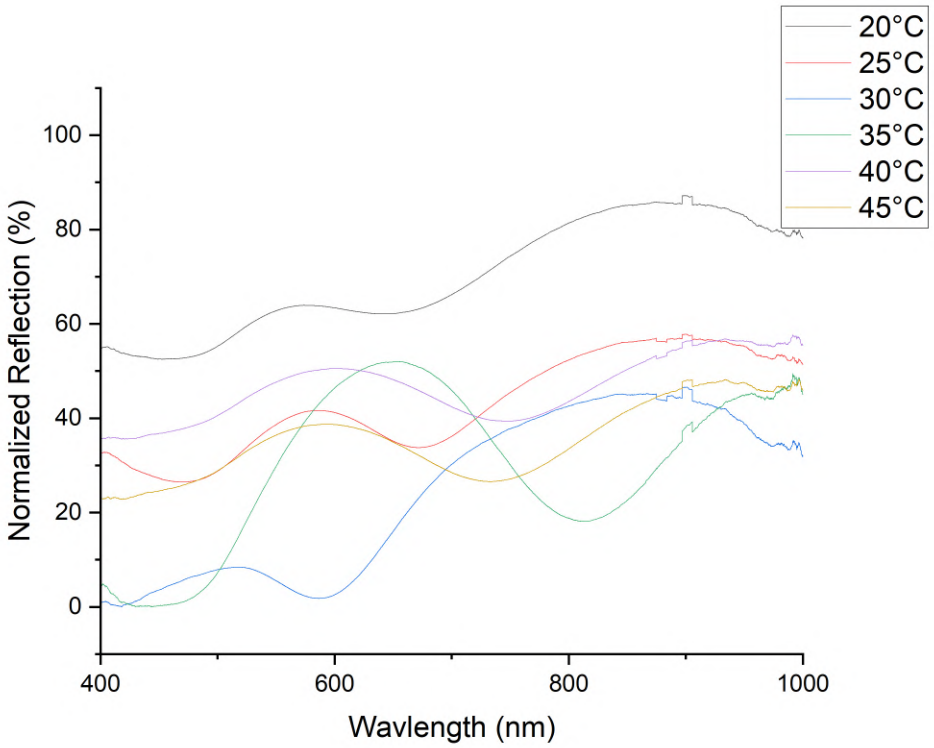

Figure A.14: 2000 DPI Normalized reflection vs Wavelength.

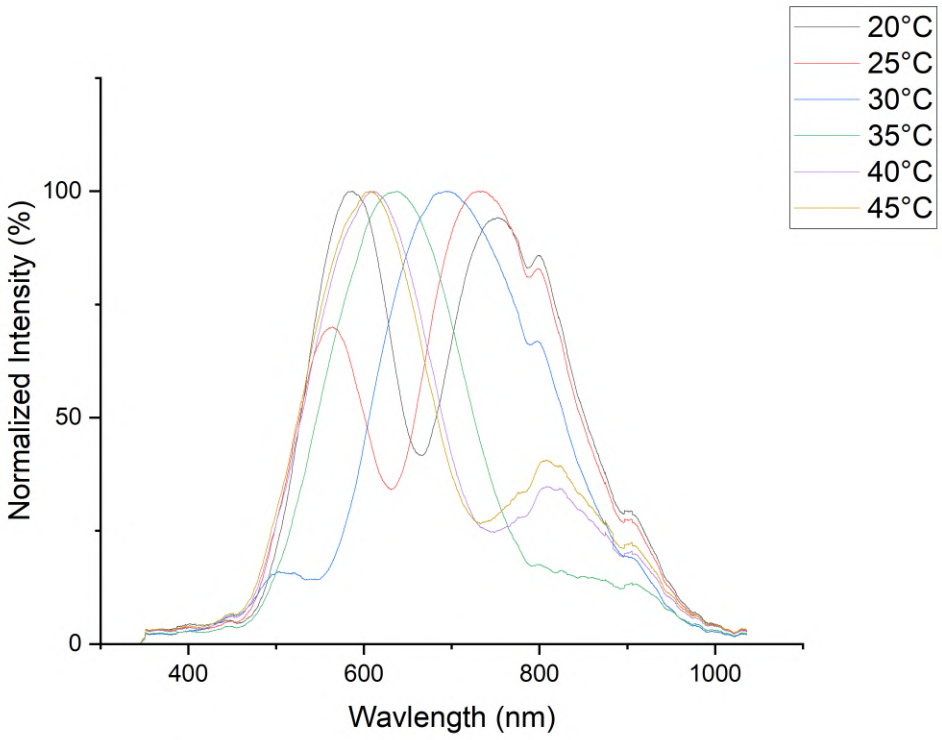

Figure A.15: 4000 DPI Normalized intensity vs Wavelength.

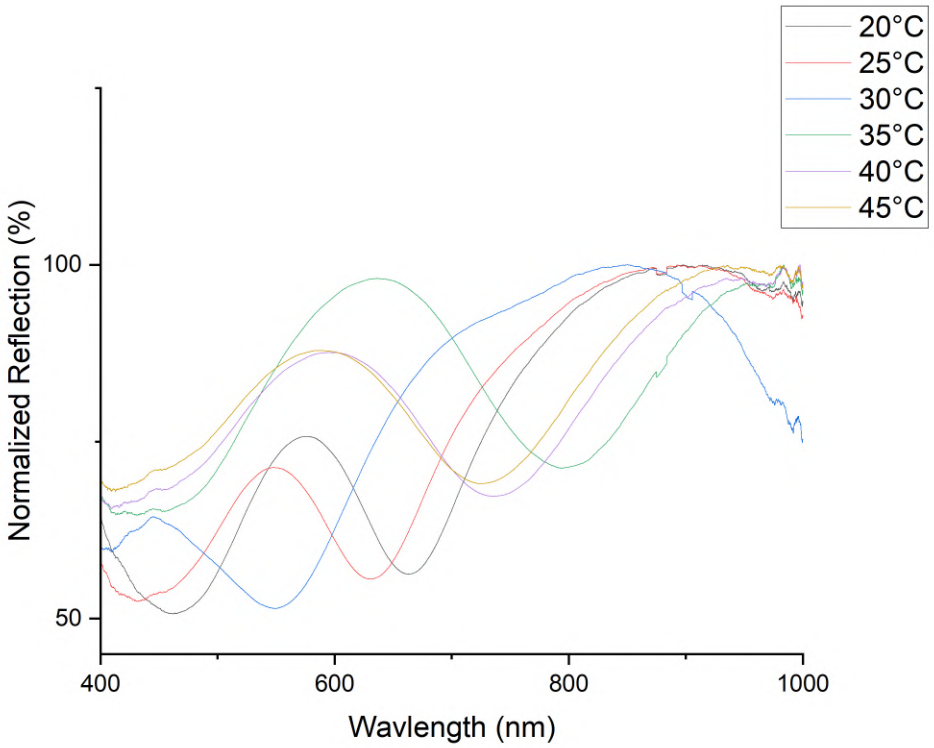

Figure A.16: 4000 DPI Normalized reflection vs Wavelength.

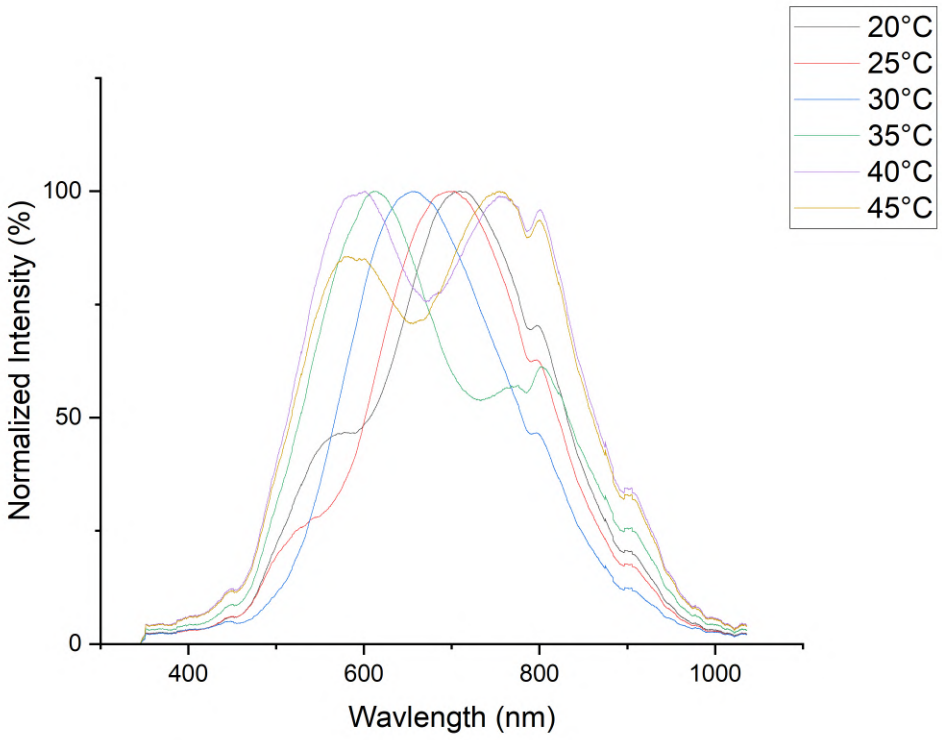

Figure A.17: 1500 DPI 2 iterations Normalized intensity vs Wavelength.

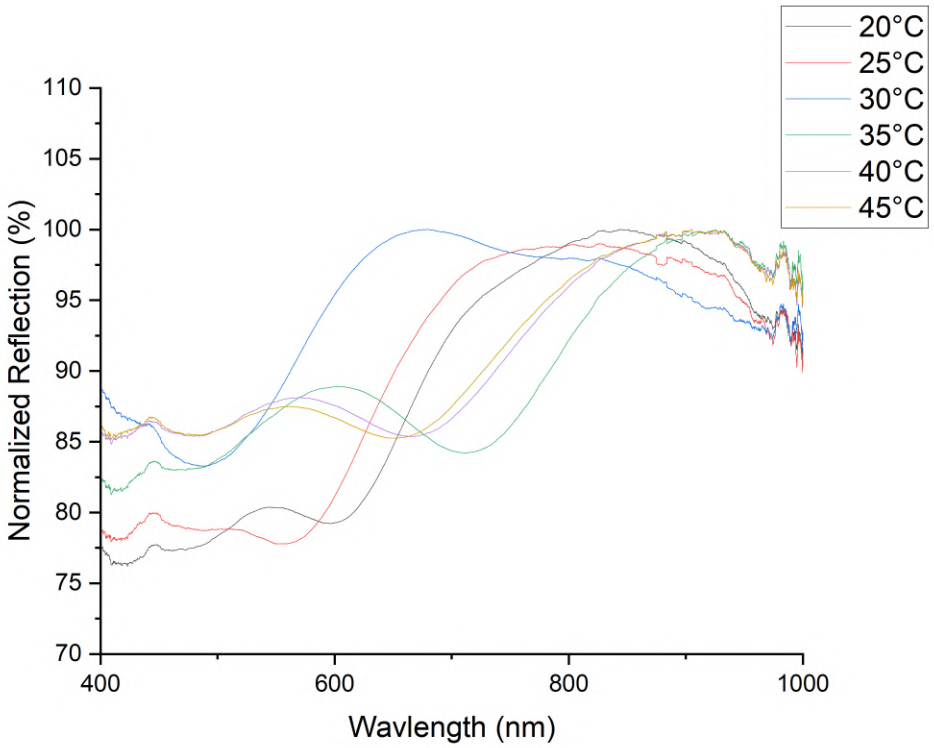

Figure A.18: 1500 DPI 2 iterations Normalized reflection vs Wavelength.